UNIVERSITY OF MINNESOTA
ST. ANTHONY FALLS HYDRAULIC LABORATORY
LORENZ G. STRAUB, Director

Technical Paper No. 30, Series B

Experimental and Analytical Studies of the Longitudinal Motions of a Tandem Dihedral Hydrofoil Craft in Regular Waves

by
J. M. WETZEL

Prepared for
DAVID TAYLOR MODEL BASIN
Department of the Navy
Washington, D.C.
under
Bureau of Ships Fundamental Hydromechanics Research Program
SR-009-01-01
Office of Naval Research Contract Nonr 710(30)

April 1960
Minneapolis, Minnesota

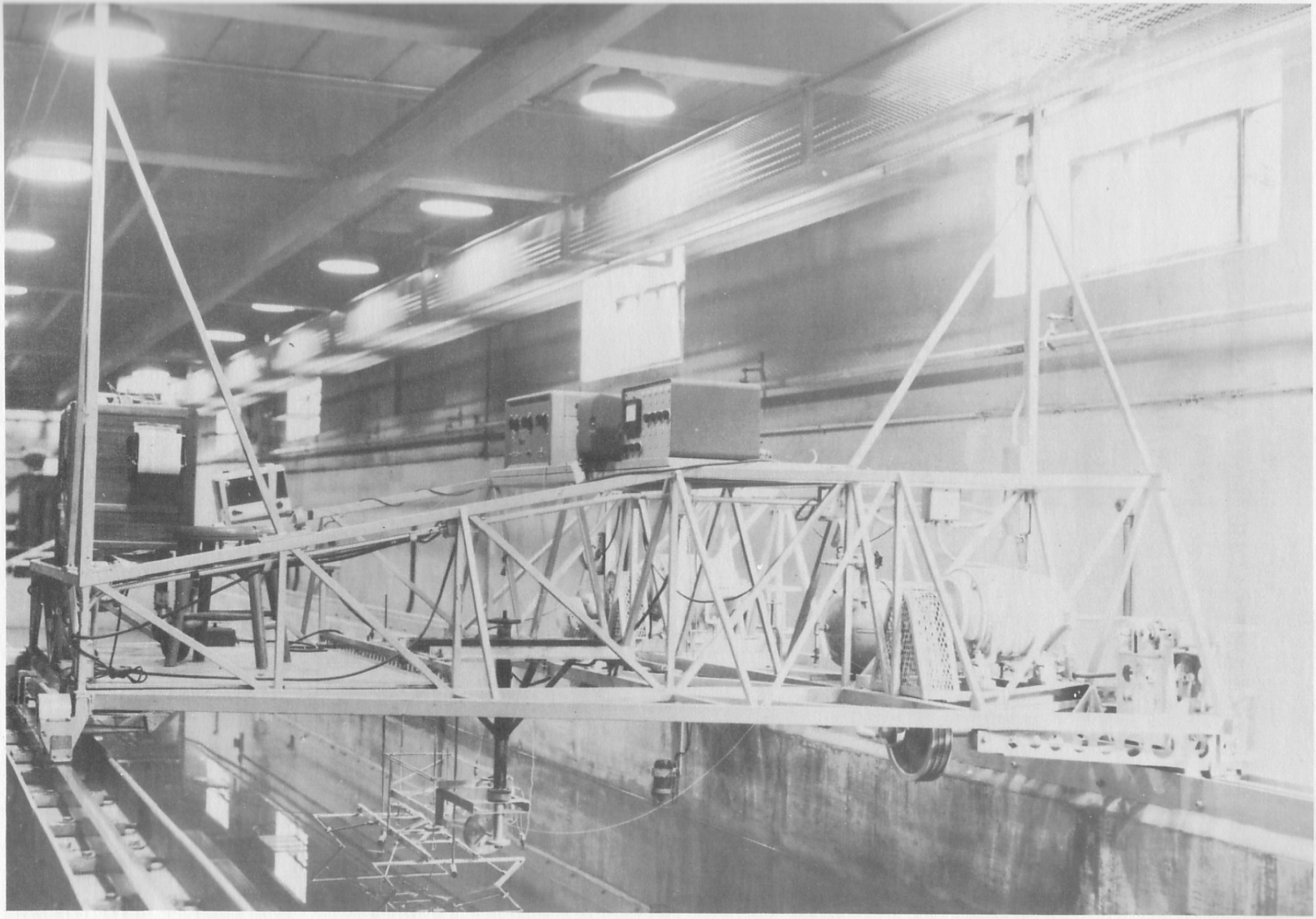

UNIVERSITY OF MINNESOTA
ST. ANTHONY FALLS HYDRAULIC LABORATORY
LORENZ G. STRAUB, Director

Technical Paper No. 30, Series B

Experimental and Analytical Studies of the Longitudinal Motions of a Tandem Dihedral Hydrofoil Craft in Regular Waves

by
J. M. WETZEL

Prepared for
DAVID TAYLOR MODEL BASIN
Department of the Navy
Washington, D.C.
under
Bureau of Ships Fundamental Hydromechanics Research Program
SR-009-01-01
Office of Naval Research Contract Nonr 710(30)

April 1960
Minneapolis, Minnesota

PREFACE

Recent nonlinear theoretical developments for the longitudinal motions of tandem dihedral hydrofoil craft in regular waves have indicated that the nonlinearities create steady components of the motions. These steady motions tend to cause the craft to crash, and are of particularly large magnitude in following seas. The studies described in this report were instigated to verify the theory in general for a wide range of wave conditions, with particular emphasis on the physical existence of the steady components predicted by nonlinear theory.

The studies were conducted during the period of November 1, 1958, to April 30, 1960. The work was carried out under the Bureau of Ships Fundamental Hydromechanics Research Program, SR-009-01-01, administered by the David Taylor Model Basin; Office of Naval Research Contract Nonr 710(30).

The entire program was under the general direction of Dr. Lorenz G. Straub, Director of the Laboratory. C. E. Bowers critically reviewed the report and developed the craft instrumentation. John Killen was primarily responsible for the analog computer solutions and also reviewed the report. D. B. Armstrong was particularly valuable in obtaining the experimental data and data reduction. K. L. Chen, L. Breimhurst, and G. Hebaus assisted in the numerical computations.

Preparation of the manuscript for printing was carried out by Marjorie Summers under the general supervision of Loyal Johnson.

A B S T R A C T

Experimental investigations were conducted with a tandem surface-piercing hydrofoil configuration free to heave and pitch in regular waves. Towing velocities of 5 and 10 fps were used in head and following seas. Tests at the lower velocity were conducted to check data previously reported by Leehey and Steele; the agreement was satisfactory. The data were compared with nonlinear and linearized theory developed by Ogilvie for both quasi-steady and unsteady conditions. The oscillatory heave, pitch, and phase relationships in general agreed well with solutions based on the linearized equations. Consideration of unsteady effects in most cases improved the correlation between theory and experiment. The primary effect of the nonlinearities was in the existence of steady components of heave and pitch. The theoretical components were verified qualitatively by the experimental results.

CONTENTS

LIST OF ILLUSTRATIONS

LIST OF SYMBOLS

A - Wave orbital motion exponential decay factor, $e^{-k\zeta}$.

A_o - First term in expansion of A, $1 - \frac{e^{-kd}}{kd}$.

a - Wave amplitude.

B_o - $c_o \rho b V^2 \cot \mu$.

B' - $c' \rho b V^2 \cot \mu$.

b - Foil chord.

$C(\nu b/2V)$ - Theodorsen function with argument $\nu b/2V$.

c - Wave celerity.

c_o - Lift coefficient for flight in smooth water.

c' - Lift curve slope.

D - Complex function that applies to unsteady foil-motion forces.

d - Depth of submergence of foil apex in smooth water.

E - Complex function that applies to unsteady orbital-motion forces.

g - Acceleration of gravity.

I - Moment of inertia of craft.

I_T - Moment of inertia of towing arm.

i - $\sqrt{-1}$.

k - $2\pi/\lambda$.

L - Lift.

ℓ - Distance to foil from c. g. of craft.

ℓ_T - Length of towing arm from pivot point.

m - Mass of craft.

r - Computer time.

t - Real time.

V - Craft velocity.

W - Craft weight, mg.

X - Modulus of D.

Y - Modulus of E.

Z - Heave displacement.

Z_o - Steady component of heave.

α - Instantaneous angle of attack.

β - Instantaneous depth of submergence.

δ - Factor equal to +1 for forward foil, -1 for aft foil.

ζ - Distance between mean position of water particle and undisturbed surface level, also argument of D.

θ - Rotation of towing arm, also argument of Y.

λ - Wave length.

μ - Dihedral angle.

ν - Frequency of encounter, $k(V \pm c)$.

ρ - Fluid density.

σ - Root of characteristic equation, also unsteady pitch phase lead.

τ - Unsteady heave phase lead.

ϕ - Phase angle, subscripts indicate heave or pitch.

ψ - Pitch.

ψ_o - Steady component of pitch (trim).

ω - Circular frequency, $2\pi/T$.

Subscripts f, a - Indicate forward or aft foil.

Subscript m - Maximum amplitude.

Symbols not included in this list are defined in the text.

EXPERIMENTAL AND ANALYTICAL STUDIES OF THE LONGITUDINAL MOTIONS OF A TANDEM DIHEDRAL HYDROFOIL CRAFT IN REGULAR WAVES

I. INTRODUCTION

Hydrofoil craft have stimulated interest in the past, although little extensive research has been conducted prior to the last decade. The continued interest in foil-supported craft is partially due to the increased speeds possible through lowered resistance, and the reduction of motions of the craft in rough water. Considerable information has been made available regarding the hydrodynamic characteristics of hydrofoils, including the influence of the free surface. It is essential that the designer of hydrofoil craft also have an indication of the performance of a given configuration in a seaway. The initial investigations of stability were concerned with flat foils which somewhat simplified the analysis. These were later extended to the dihedral or area-stabilizing foils. Little experimental data are available to verify existing theories. Leehey and Steele [1] have reported the only systematic tests that could be used to verify theoretical work prior to the current tests described in this report. Their tests were conducted only for a rather limited number of wave conditions and in a relatively narrow towing facility. As some question existed as to the reliability of the data due to instrumentation techniques and the test facility, it was desired to check these results and extend the data to cover a wider range of wave characteristics and also a higher towing speed. The St. Anthony Falls Hydraulic Laboratory has continued this investigation under terms of Contract Nonr 710(30). The following report describes the results of the program. Some earlier results of this investigation have been previously reported in Memorandum No. M-80 [2]. These preliminary results are superseded by the present report.

II. THEORETICAL CONSIDERATIONS

The prediction of the longitudinal motions of a hydrofoil craft in regular waves was considered by Weinblum [3] some time ago. To expedite calculation of the equations, he considered only the linear terms which resulted in an approximate and simplified solution to the problem. It was found by

Leehey and Steele that the experimental data did not agree well with the linearized theory. The theoretical motions were considerably greater than the experimental. The discrepancy was attributed primarily to the linearization and quasi-steady assumptions. Ogilvie [4] has extended Weinblum's work to include the exponential decay of the wave orbital motion and the effects of unsteadiness. The equations were also retained in their nonlinear form. Even when the effects of unsteadiness and nonlinearities were neglected, it was found that the correlation between the theory and experiment was improved, primarily by the consideration of decay of orbital velocity with depth. The solutions of the nonlinear equations further indicated that a steady displacement of heave and pitch existed that was dependent on the wave amplitude. The craft did not oscillate about its flight position in smooth water, but about a level displaced downward from this position. This displacement was particularly large for following seas, where in some cases it actually exceeded the oscillatory amplitude. The prediction of the steady component is of particular importance, as some difficulties have been reported with prototype craft in following seas. The steady component would not, of course, be observed in solutions of the linearized equations.

The analysis developed by Ogilvie was restricted to a system free to heave and pitch as shown in Fig. 1. To simplify the equations of motion, it was first desired to make several assumptions regarding the lift on a surface-piercing foil in waves. Many of the assumptions were later investigated to determine their validity. The following restrictions were imposed in calculating the lift:

1. The lift is proportional to the product of the instantaneous angle of attack and the instantaneous horizontal projection of the submerged foil area.
2. The wave length is much greater than the foil chord.
3. The slope of the lift curve is constant.
4. The downwash and waves generated by the forward foil may be neglected.
5. The horizontal component of the wave particle motion is small compared to the craft speed.
6. The distance from the center of gravity of the craft to the foil is much greater than the foil chord.

These assumptions indicate that the quasi-steady case was considered. The added mass effects were then included with consideration of other unsteadiness. The drag pitching moment was not included in the equations.

With the previous assumptions, the quasi-steady lift on each foil was calculated and substituted in the equations of motion for two degrees of freedom:

$$m\ddot{Z} = \sum_{f,a} L - W \tag{1}$$

$$I\ddot{\psi} = \ell_f L_f - \ell_a L_a \tag{2}$$

The results of this substitution are

$$m\ddot{Z} = 1/2\,\rho\,V^2 \sum_{f,a} \Big[\overbrace{(2b \cot \mu)[d - Z - \delta \ell \psi + a \cos(\nu t + k \delta \ell)]}^{①} \Big\{ c_o + c' \big[\overbrace{\psi - 1/V (\dot{Z} + \delta \ell \dot{\psi} \pm a \omega A \sin(\nu t + k \delta \ell))}^{②} \big] \Big\} \Big] - W \tag{3}$$

$$I\ddot{\psi} = 1/2\,\rho\,V^2 \sum_{f,a} \Big[\delta \ell \overbrace{(2b \cot \mu)[d - Z - \delta \ell \psi + a \cos(\nu t + k \delta \ell)]}^{①} \Big\{ c_o + c' \big[\overbrace{\psi - 1/V (\dot{Z} + \delta \ell \dot{\psi} \pm a \omega A \sin(\nu t + k \delta \ell))}^{②} \big] \Big\} \Big] \tag{4}$$

where m = mass of craft,

Z = heave,

L = lift on foils,

W = weight of craft,

I = moment of inertia of craft,

ψ = pitch,

ℓ = distance to foil from center of gravity of craft,

ρ = fluid density,

V = craft velocity,
b = foil chord,
μ = dihedral angle,
d = depth of submergence,
a = wave amplitude,
ν = frequency of encounter, $k\,(V \pm c)$,
$k = 2\pi/\lambda$,
c_o = lift coefficient for flight in smooth water,
c' = lift curve slope, and
ω = circular frequency.

In these equations, $\delta = +1$ for the forward foil designated by the subscript f, and $\delta = -1$ for the aft foil designated by subscript a. The summation sign indicates that each of the variables for the forward and aft foil should be added together. Whenever a double sign appears, it is understood that the upper sign refers to head seas and the lower sign to following seas. The variables are also given in the List of Symbols.

The terms included in the brace ① represent the instantaneous projected foil area, and in brace ② the instantaneous angle of attack. The factor, A, takes into account the mean value of the exponential decay of the orbital motion over the depth of the foil and is given by

$$A \equiv \overline{e^{-k\zeta}} = 1 - \frac{e^{-kd}}{kd}\,[1 + \text{const}\,(Z + \delta \ell \psi) + \cdots]$$

The first term of this expansion, A_o, corresponds to the mean value for no oscillation. Inclusion of this factor results in roughly a two-fold reduction of craft motion and greatly improves the correlation with experiment as will be seen in later sections.

Equations (3) and (4) were simplified by linearization. Assuming that craft motions and wave amplitudes were small, all quadratic and cross product terms of the variables Z, ψ , and a were dropped from the equations. As it was of interest to determine the validity of the linearized equations, solutions are presented in Appendix A.

The effect of removing several of the quasi-steady assumptions was also considered for the linearized equations. In general, Ogilvie carried

out the analysis by appealing to classic two-dimensional aerodynamic gust theory, and applying it to the hydrofoil case with the assumption that the finite foil was affected by unsteadiness in the same manner as the infinite wing.

Unsteadiness corrections have been applied to the following quantities that comprise the lift on a foil.

1. Pitch and vertical motions of the foil, and
2. Change of angle of attack due to wave orbital motions through consideration of nonuniform velocity distribution over the chord.

The unsteadiness associated with change in depth and consequently change in area of the surface-piercing foil was not considered. No comparable situation exists in aerodynamic theory, and based on difficulties or complexities experienced in calculating unsteady lift forces on flat hydrofoils near the surface [5], this source of unsteadiness was neglected. This may not be justified for following seas where the change in area may be appreciable.

By analogy to airfoil theory, it was possible to reduce the effect of unsteadiness to a product of the quasi-steady lift with a function dependent on the reduced frequency. For example, the unsteady lift associated with the foil motions was composed of two parts, one of circulatory origin and the other of noncirculatory origin. The former takes into consideration the wake vorticity, and is found from the product of the quasi-steady lift and the well-known Theodorsen function. The component of noncirculatory origin is attributed to added mass effects which were not considered in the quasi-steady case. The unsteady functions are defined and plotted in Appendix A.

Calculations were also made concerning the effects of the horizontal component of orbital velocity and downwash on the motions. As expected, the horizontal velocity component became of decreasing importance as the craft speed increased. For the higher towing velocities, this correction should be negligible. The downwash was calculated by considering the vertical velocities induced at the aft foil by the vorticity of the forward foil, and assuming that the vorticity decayed in a manner similar to that generated by a cylinder. For a particular condition, a calculation was made that indicated the effect of downwash could probably be safely neglected. The subject of

the downwash generated by a dihedral foil piercing the free surface apparently requires more extensive investigation.

III. EXPERIMENTAL APPARATUS AND PROCEDURE

A. Test Facility

The tests were conducted in the multi-purpose channel which is 9 ft wide, 6 ft deep, and 220 ft long. The water depth was maintained at 4.5 ft. This facility is equipped with a self-propelled towing carriage and a wave generator. The towing carriage is capable of attaining accurately controlled speeds in either direction up to a maximum of 25 fps. Speeds of 5 and 10 fps were used for the current tests. The wave generator will provide waves of various lengths and amplitudes, up to a maximum of about 18 ft long and 2 ft high. Waves down to about 2.8 ft in length can be generated satisfactorily. Below this value, the waves become unstable as they proceed down the channel, thereby reducing the length of the test run. For this reason, lengths shorter than 2.8 ft were not used in the tests. A permeable-beach absorber was located at the opposite end of the channel to minimize wave reflections. A more complete description of the facility is presented in a current technical paper [6].

B. Hydrofoil Craft

The hydrofoil craft was obtained on loan from the sponsor and was the same one as previously used by Leehey and Steele. The tandem "V" foil configuration consisted of two aluminum 45-degree dihedral foils of 2-in. chord with a Wright 1903 section. The two foils were spaced 3 ft apart, equal distances from the center of gravity. The construction of the original craft and towing arm was such that the heave and pitch were not measured independently. The signals generated by micropotentiometers driven by a gear-rack arrangement were subtracted electronically to permit recording of the actual heave and pitch traces with respect to a fixed reference. At the request of the sponsor, the instrumentation system was changed to permit an independent check of the existing data. All axle bearings were also replaced. The original and modified systems are shown schematically in Fig. 2. Note that in Fig. 2a the entire towing arm, including the member supporting the craft, was free to rotate. The elements of the towing arm were then revised to form a

parallelogram, thereby permitting the measurement of heave and pitch independently. Linear differential transformers replaced the micropotentiometers as the sensing elements. The heave indicator was fastened to the towing arm and the rigid towing strut attached to the carriage. The pitch indicator was fastened to the craft and the vertical member supporting the craft axle. The parallelogram arrangement permitted only a vertical movement of this member. The movable weights made possible the adjustment of the center of gravity and moment of inertia. The centers of gravity of the towing arm and craft were located at their pivot points. Photographs of the revised craft and also of the craft attached to the carriage are shown in Fig. 3 and the frontispiece.

After alterations of the instrumentation system were made, the weight and moment of inertia were adjusted to be the same as the original craft to provide direct comparison of the data by Leehey and Steele. The moment of inertia of the craft was measured both with the Bifilar method and the method described by Reiss [7]. The agreement between the two methods was satisfactory.

The towing arm was carefully balanced about its pivot point so that none of its weight would affect the craft responses. The moment of inertia of the towing arm was determined to permit corrections to be calculated for the comparison of experimental and theoretical responses. The measured moment of inertia was 0.34 slug ft^2. The calculation of the correction is given in Appendix B. The correction was applied to the heave equation and appeared to be most significant in the heave phase relationships for the smaller wave lengths.

The craft was found to be structurally deficient at a towing velocity of 10 fps, as it was not designed to be towed at this speed. It was thus necessary to add additional members to the framework and foils, and as the weight and moment of inertia were not corrected for the addition of such braces, these values will be different from those at 5 fps. Some of this bracing can be seen in Fig. 3 and the frontispiece. A summary of the characteristics of the craft at an equilibrium condition in smooth water for velocities of 5 and 10 fps is tabulated in Table I.

TABLE I

	V = 5 fps	V = 10 fps
Displacement, lbs	4.02	4.56
Moment of Inertia, slug ft^2	0.151	0.168
Average Lift Coefficient	0.456	0.171
Lift Curve Slope	4.41	4.65
Foil Submergence, ft	0.55	0.42
Distance from c. g. to either foil, ft	1.5	1.5

The wave profile was measured in early tests with a capacitative wave recorder. This was later replaced with the sonic surface wave transducer as developed at this Laboratory [8]. The sonic transducer greatly reduced the difficulties created by dust on the water surface in measuring wave heights accurately. Both the capacitive probe and the sonic head were mounted directly opposite the center of gravity of the craft to permit ease in calculation of phase relationship between the wave and craft motions. The measurements of carriage speed, heave, pitch, and the wave profile were recorded with a consolidated oscillograph. The wave length was calculated from the known period of the generator paddle.

C. Test Procedure

Steady-state lift measurements were made at 5 and 10 fps for various angles of attack and submergences to permit determination of the lift-curve slope required in the theoretical analysis.

The craft was adjusted to fly at nearly zero heave and trim at a given velocity and submergence in smooth water. Compensations were made in the angle of attack to correct for the drag diving moment not included in the theory. Waves were generated with lengths from 2.6 to 15 ft and heights from 0.05 to 0.4 ft. The shorter waves at the larger amplitudes could not be generated satisfactorily, as the waves become unstable after traveling some distance. At a craft velocity of 5 fps, waves longer than 3.5 ft could not be used for following seas as the craft crashed onto the surface. To avoid crashing at a craft velocity of 10 fps, tests were restricted to waves up to 7.5 ft long and with low amplitudes. After the first crash occurred, it was deemed

desirable to provide limit stops to restrict the amplitude of the motions, thereby preventing damage to the craft. These limit stops were placed as close as possible to the wave crests and consisted of 1-in. diameter tubes which were later flattened to 1/4 in. thick.

The craft was supported at its approximate equilibrium position and released shortly after the acceleration run. In some cases the craft was permitted to "take off" by itself. Little discrepancy was noted between the two methods of starting. As a matter of interest, several runs were made with the craft overtaking or meeting waves from a start in smooth water. For head seas, the craft had attained its flight position in smooth water before meeting the oncoming waves. For following seas, the wave generator was stopped, the craft attained its equilibrium position in smooth water, and it overtook the wave train. The response of the craft for both cases was satisfactory.

D. Data Reduction

Records were obtained of the following variables: 1) wave profile at center of gravity of craft, 2) heave, 3) pitch, and 4) towing speed.

Typical test records for following and head seas are shown in Fig. 4 for towing velocities of 5 and 10 fps, respectively. Each trace is properly labeled to provide identification for reference purposes.

After Ogilvie, the data have been plotted in terms of dimensionless parameters which are defined below:

heave amplification factor = Z_m/a
pitch amplification factor = $\psi_m \ell/a$
nondimensional steady heave = Z_o/a
nondimensional steady pitch = $\psi_o \ell/a$

where Z_m = maximum heave amplitude,
Z_o = steady heave displacement measured from smooth water flight position,
ψ_m = maximum pitch amplitude,
ψ_o = steady pitch (trim) measured from smooth water flight trim,
ℓ = distance of foils from center of gravity of craft, and
a = wave amplitude.

These values are shown in the typical test records. The heave phase lead ϕ_Z is defined as the amount in degrees of wave cycle that the maximum upward craft heave leads the wave crest at the center of gravity of the craft. The pitch phase lead ϕ_ψ is defined as the amount in degrees of wave cycle that the maximum bow up pitch leads the crest of the wave at the center of gravity of the craft.

Note that the steady component of heave is measured from the equilibrium flight position. This position is shown by the broken line, and is an average value for a number of runs in smooth water. The maximum discrepancy between the value for a particular run and the average value was 8 per cent. The steady pitch in Fig. 4b is bow up. The steady pitch in most cases was rather small, and no reliable trends could be determined between successive runs.

IV. DISCUSSION OF RESULTS

A. Transient Response

The longitudinal stability of the craft in smooth water has been determined from the linearized equations of motion. As the roots of the characteristic equation were negative, the craft was inherently stable. (The roots are given in Appendix A.) The response of the craft to an initial disturbance at a velocity of 5 fps as reported by Leehey and Steele indicated that the theory was conservative in predicting the response. Experimental transient responses for initial values of pitch and heave at a velocity of 10 fps are shown in Fig. 5. The same type of behavior is found in that the actual motions are more rapidly damped than expected.

B. Oscillatory Motions

As previously mentioned, the first task with the modified craft as shown in Fig. 2b was to verify the data taken by Leehey and Steele. The results of this investigation are presented in Figs. 6 through 9 for head seas and Figs. 10 through 13 for following seas. The agreement of the data from TMB and SAFHL was satisfactory, and for this reason only data taken at this Laboratory have been plotted. The calculated curves have been taken from Ogilvie's paper for wavelengths less than 5 ft in head seas. Curves for other wave lengths were calculated from the solutions given in Appendix A. The

theoretical and experimental motions are in general in good agreement. It appears that heave is more difficult to predict than pitch. Referring to Fig. 6, the experimental data are displaced somewhat above the theoretical curves for wave lengths of 3 ft and greater than 5 ft. The unsteady calculation improves correlation but is not entirely sufficient. The experimental heave phase lead in Fig. 7 differs from the quasi-steady calculations by about 20 degrees for the shorter wave lengths. Pitch and pitch phase agreement with theory is good except at a wave length equal to the foil spacing (3 ft) where the theoretical condition of zero pitch is not completely realized, although only small pitches were measured. The effect of nonlinearities was also small for head seas.

In following seas, Figs. 10 through 13, the nonlinear calculations tend to agree better with experimental data. This is probably to be expected, as noting the change in ordinates for these plots, the craft motions are considerably greater than for head seas. The data were limited to wave lengths less than about 4.0 ft, as the craft crashed for waves exceeding this length. Even at the longest wave length, it was necessary to restrict the wave amplitude to less than about 0.05 ft.

The oscillatory heave and pitch data for a towing velocity of 10 fps are shown in Figs. 14 through 21 for head and following seas. The various points for each wave length indicate the influence of wave amplitude on the dimensionless parameters. In general, it was found that the dimensionless amplification factors tended to decrease with increasing wave amplitude. However, the quasi-steady theory appears to be adequate in predicting the motion in most cases. In Fig. 15, it will be noted that the data for the 4-ft wave length differs from theory by about 50 degrees. The values were rechecked, but no obvious error was found. For other wave lengths, the theory seems adequate. The consideration of the effects of unsteadiness tends to improve correlation with the experimental data. The towing arm correction described in Appendix B has been applied to all heave calculations, with the only significant change being in the phase relationship for small wave lengths.

The linear quasi-steady pitch calculation, Fig. 16, appears to be somewhat conservative for the wave lengths exceeding 6 ft. When unsteadiness effects are included, the agreement between theory and experiment is improved.

Again the condition of zero pitch was not attained for a 3-ft wave length, although the pitch was small in this region.

The linearized theory was also satisfactory in most cases for following seas as seen in Figs. 18 through 21. Attention is again called to the change in scale for these graphs, as the amplification factors are considerably greater than in head seas. The maximum wave length was limited to prevent crashing, and for the points shown it was necessary to restrict the wave amplitude to less than about 0.05 ft. The heave phase lead, Fig. 19, for waves less than 4 ft is about 15 degrees less than predicted.

For the longer wave lengths, the measured pitch response, Fig. 20, was somewhat greater than the theoretical. Unsteady conditions did not improve correlation in this case.

C. Steady Components of Heave and Pitch (Trim)

The nonlinear theory indicated that the oscillation of the heave and pitch would occur about a position displaced downward from the mean flight level in smooth water. Up to this time, no experimental data were available to compare with this theory. The experimental displacement proved difficult to measure, and some of the results for a towing velocity of 5 fps in following seas are shown in Fig. 22. The curves are analog solutions obtained from Ogilvie's paper for several wave amplitudes. The experimental data were taken for several different amplitudes as indicated in the legend. The data agree fairly well with the predicted values, in most cases following at least the general trends. Some difficulty was encountered in attempting to measure the displacement. Under many conditions, a zero shift occurred, but it was not a steady displacement. Rather, the zero shifted downward and oscillated with a period considerably longer than the wave period. This period was also found to vary with wave length and slightly with wave amplitude. The data shown in Fig. 22 were taken from records that were free of this oscillation. Typical values of the period for various wave conditions are shown in Table II.

TABLE II

Wave Length, ft	Wave Amplitude, ft	Period of Displacement, sec
2.6	0.018	1.75
2.9	0.028	2.5
2.9	0.18	1.75
4.1	0.048	7.5
4.4	0.079	9.0
4.6	0.049	15.0
4.6	0.074	11.0
5.6	0.068	12.0
6.0	0.112	4.25
6.0	0.046	13.5

In an effort to eliminate this oscillation, considerable time was allowed between successive tests for the tank to settle out. As it was suspected that a change in velocity may result in such an oscillation, a continuous record of the towing velocity over the entire run was also made which is shown in the test records in Fig. 4. This record did not show any measurable changes in towing velocity.

As time did not permit an exhaustive study of the long period oscillation, tests were conducted at a velocity of 10 fps. At the higher speed, less tendency was noted for the craft to oscillate at these long periods. A limited number of data points were obtained in following seas. It was not possible to utilize a number of wave amplitudes as the craft crashed for even relatively small amplitudes and the longer wave lengths. The available data can be seen in Fig. 23. The experimental data can be determined from the legend, and the analog computer solutions are shown by the solid curves. The smallest amplitude (0.34 in.) has considerable scatter at the 3-ft wave length. Although the data have some scatter, in general the trends of the data agree satisfactorily with theory.

The results for head seas are shown in Fig. 24 for four wave amplitudes. The analog solutions are shown with the solid line. Broken lines through symbols represent experimental data. It was found that in general the correspondence with theory increased with increasing wave amplitude. Part

of this may be associated with the inaccuracies in measurement that may exist for the smaller amplitudes, which are somewhat amplified by the parameter Z_o/a. A deviation from theory which at the present time cannot be explained appears in all cases to occur between wave lengths of 6 to 10 ft. Little change is noted in the theoretical Z_o/a for the longer wave lengths and a given wave amplitude. The effect of wave length on the coefficients of the forcing function is relatively small for the longer waves.

Considering the difficulty experienced in determining the steady displacement, the correlation with theory is rather good. Of course, other sources of nonlinearities neglected in the theory could be included that may alter the correlation somewhat. The nonlinearities considered have been mentioned in a previous section.

The measurement of the steady component of pitch was not very successful as scatter could not be sufficiently reduced for reliable trends to be established. The steady pitch in most cases was of a very small value that made accurate measurement difficult. In observing the behavior of the craft in following seas, it seemed that the craft would make several oscillations and then suddenly assume a bow down attitude from which it would not recover. It appeared that the drag moment was increased considerably. This effect could be attributed to a combination of the steady downward components of heave and pitch, although the latter was difficult to distinguish.

V. CONCLUSIONS

The following conclusions can be made based on the experimental results described in this report for a tandem "V" hydrofoil configuration.

1. The data previously reported by Leehey and Steele and the current SAFHL data agreed satisfactorily for the towing velocity of 5 fps.

2. The experimental response to an initial disturbance is more heavily damped than indicated by theory.

3. The SAFHL data in general qualitatively verify the quasi-steady theory developed by Ogilvie.

4. The consideration of unsteady effects modifies the results slightly, and in most cases the additional effort

in calculation may not warrant their consideration.

5. The significant effect of nonlinearities is in the theoretical prediction of steady components of heave and pitch. The experimental data indicate that such components exist, although a discrepancy is noted between theory and experiment for small wave amplitudes. Agreement is improved with the larger amplitudes.

6. The tandem "V" foil configuration has a tendency to crash in following seas for the physical conditions used in these tests. The tendency to crash is reduced with increasing craft velocity or frequency of encounter.

LIST OF REFERENCES

[1] Leehey, Patrick, and Steele, J. M. Jr. Experimental and Theoretical Studies of Hydrofoil Configurations in Regular Waves. David Taylor Model Basin Report 1140, October 1957.

[2] Wetzel, J. M., and Armstrong, D. B. Experimental Studies of a Tandem Dihedral Hydrofoil Configuration in Regular Waves. University of Minnesota, St. Anthony Falls Hydraulic Laboratory Memorandum No. M-80, August 1959, 24 pages.

[3] Weinblum, G. P. Approximate Theory of Heaving and Pitching of Hydrofoils in Regular Shallow Waves. David Taylor Model Basin Report C-479, October 1954.

[4] Ogilvie, T. Francis. The Theoretical Prediction of the Longitudinal Motions of Hydrofoil Craft. David Taylor Model Basin Report 1138, November 1958.

[5] Kaplan, Paul. Longitudinal Stability and Motions of a Tandem Hydrofoil System in a Regular Seaway. Stevens Institute of Technology, Davidson Laboratory Report No. 517, December 1959, 43 pages.

[6] Straub, Lorenz G., and Bowers, C. E. The St. Anthony Falls Multi-Purpose Test Channel. University of Minnesota, St. Anthony Falls Hydraulic Laboratory Technical Paper No. 17, Series B, July 1956.

[7] Reiss, Howard R. A Procedure to Impart Specified Dynamical Properties to Ship Models. David Taylor Model Basin Report 986, March 1956.

[8] Killen, John M. The Sonic Surface-Wave Transducer. University of Minnesota, St. Anthony Falls Hydraulic Laboratory Technical Paper No. 23, Series B, July 1959, 31 pages.

[9] Fung, Y. C. An Introduction to the Theory of Aeroelasticity. John Wiley and Sons, Inc., 1955.

F I G U R E S

(1 through 24)

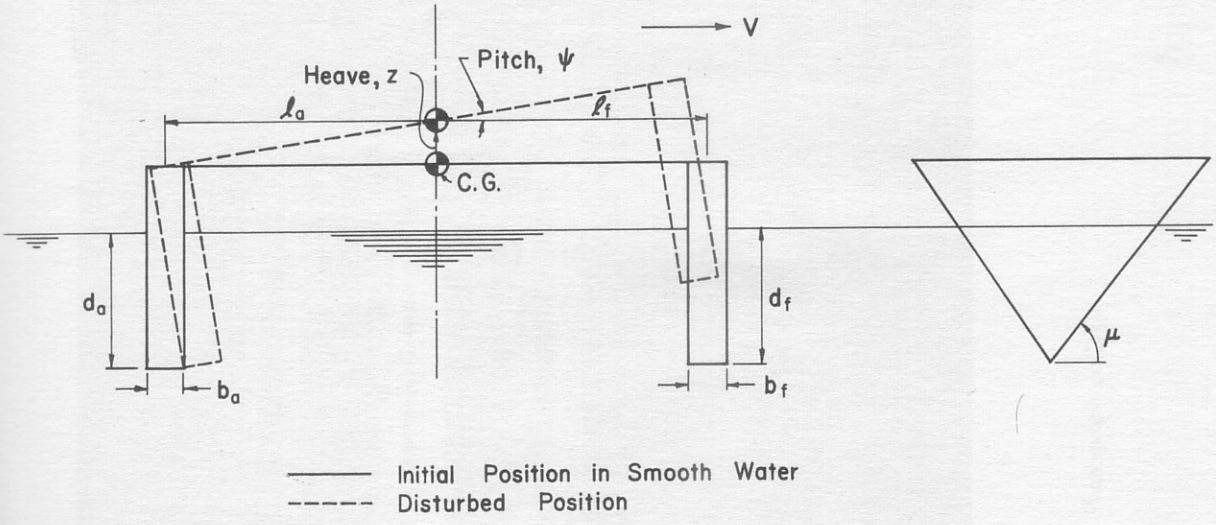

Fig. 1 - Definition Sketch of Craft Geometry

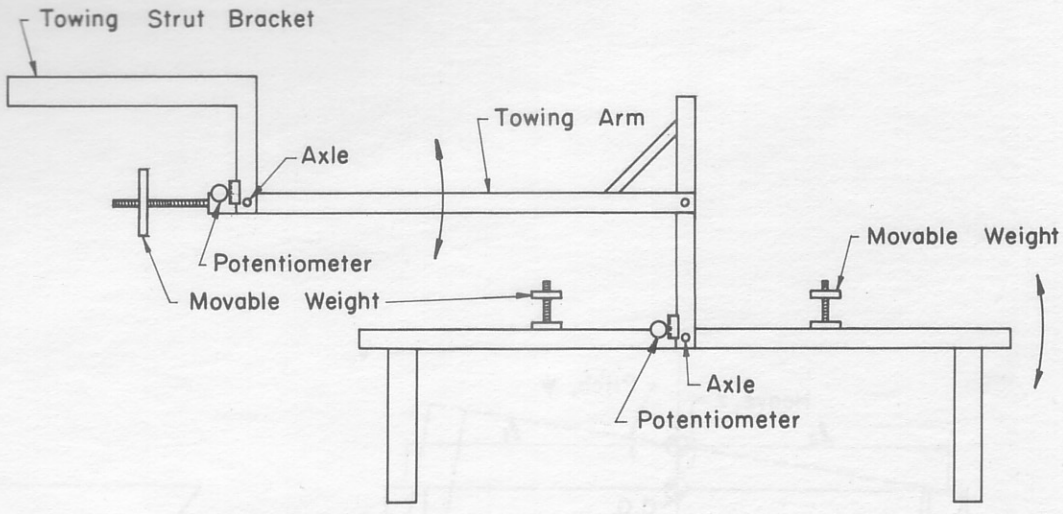

(a) Original (DTMB)

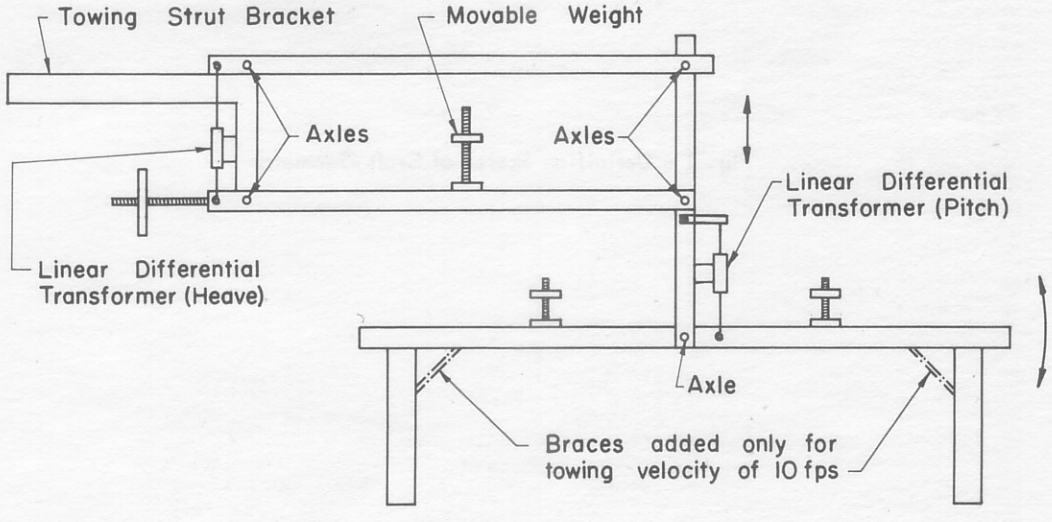

(b) Modified (SAFHL)

Fig. 2 - Instrumentation of Hydrofoil Craft

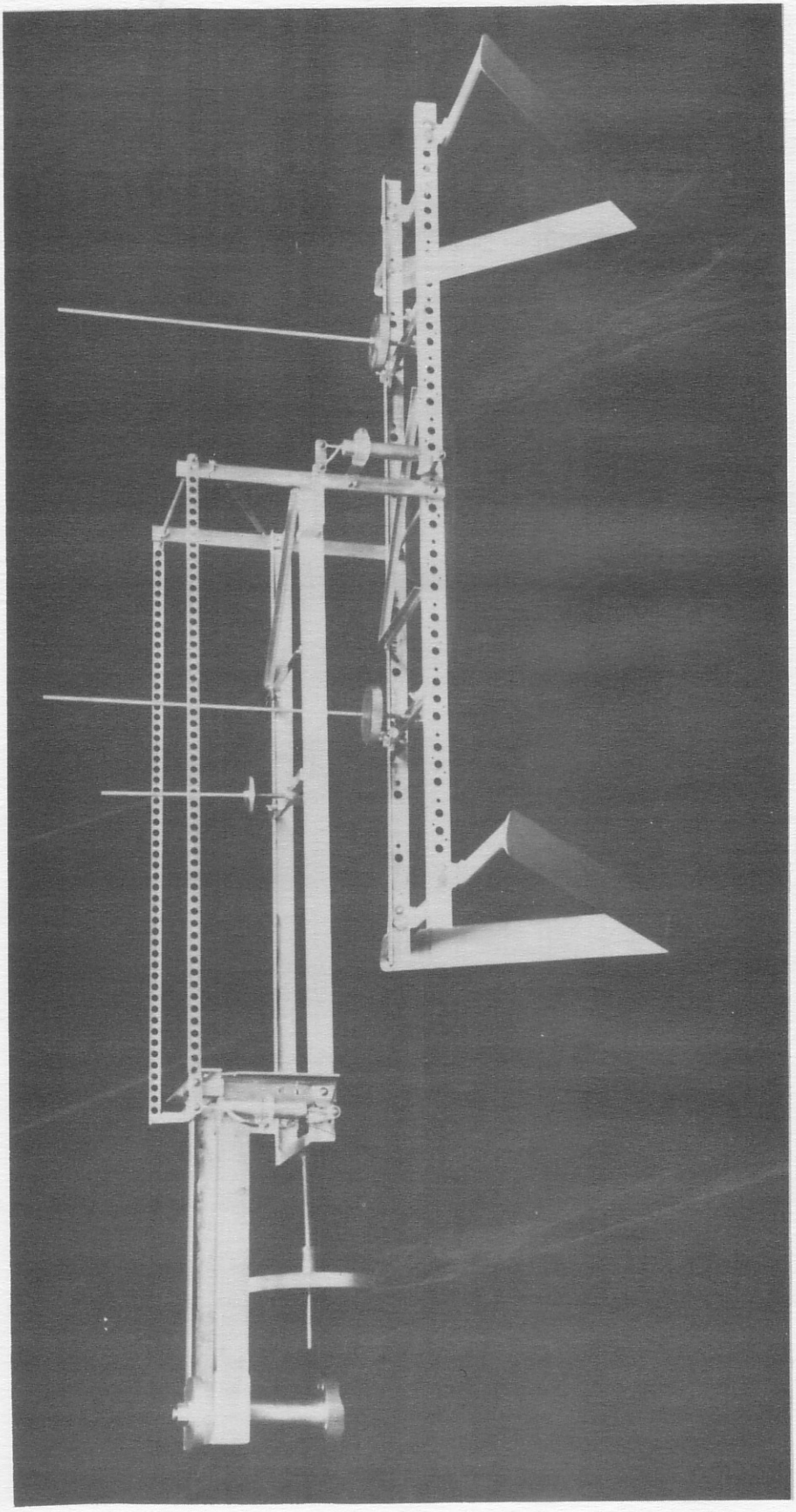

Fig. 3 – Photograph of Craft

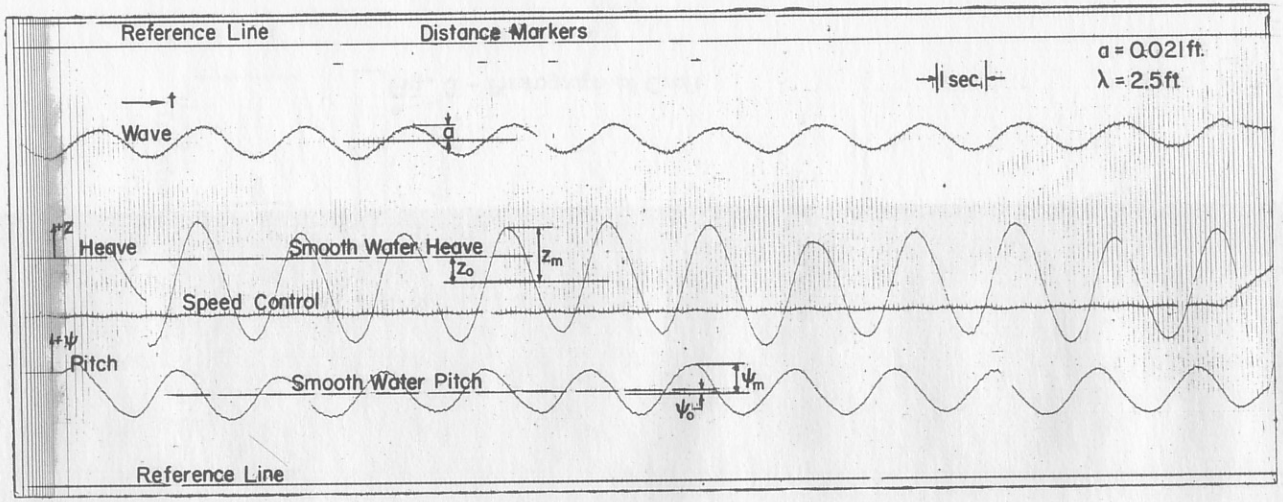

a. Following Seas, V = 5 fps

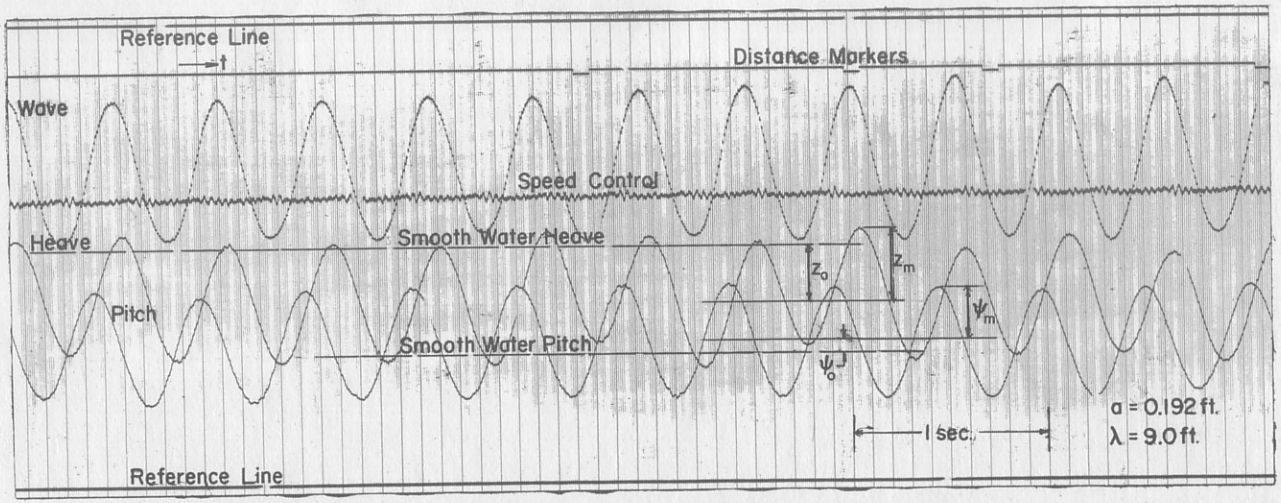

b. Head Seas, V = 10 fps

Fig. 4 – Typical Test Records

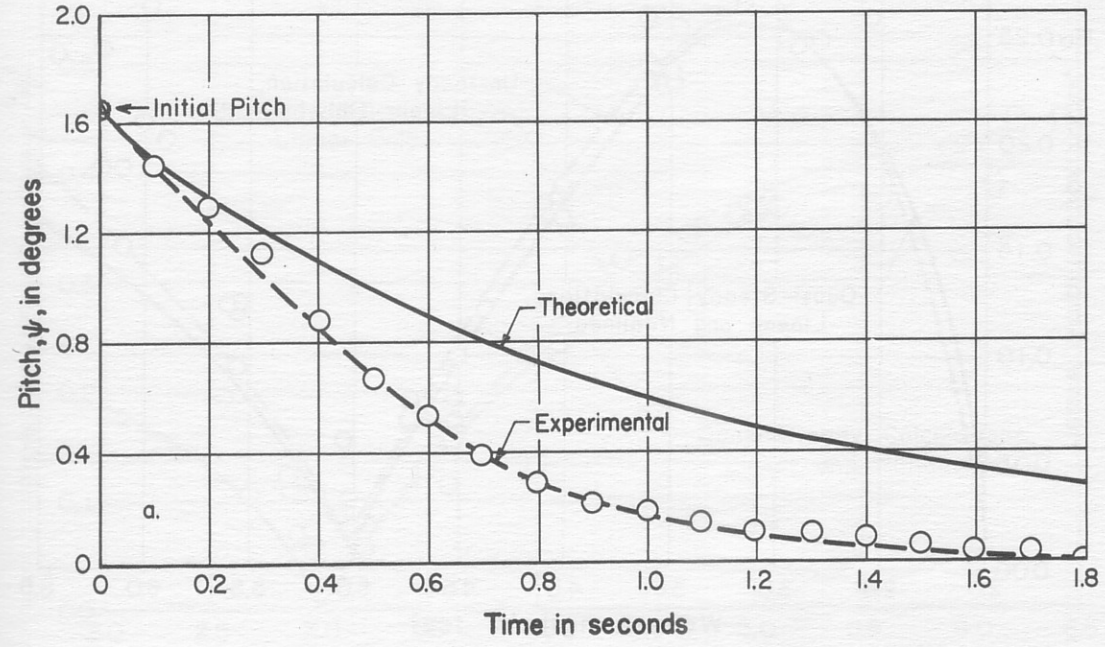

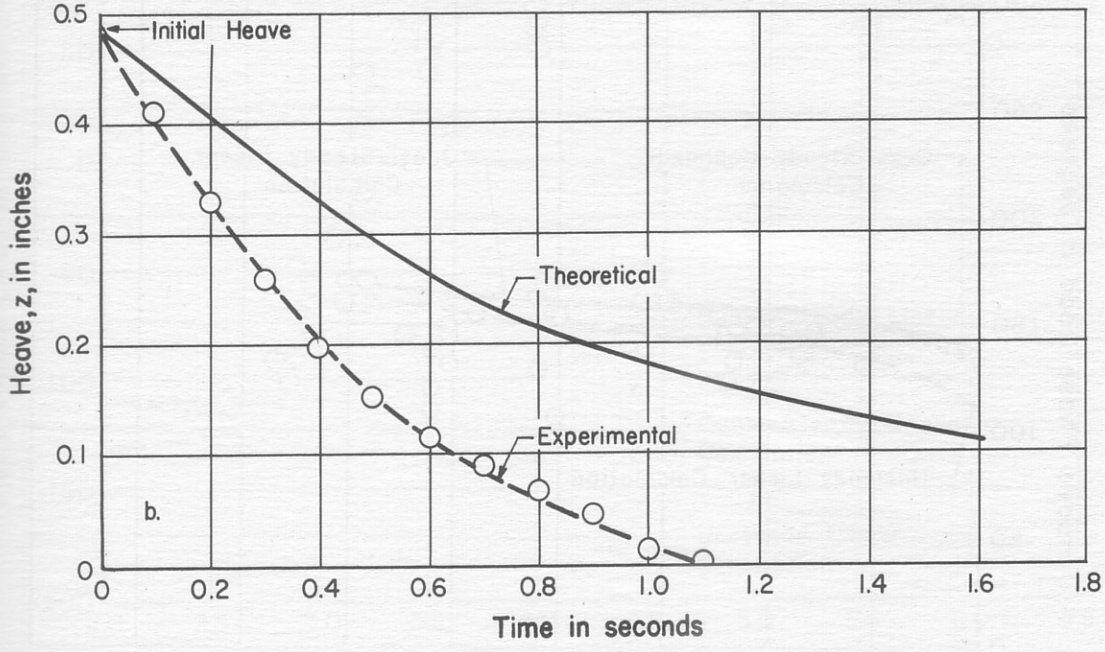

Fig. 5 – Craft Response to Initial Displacement

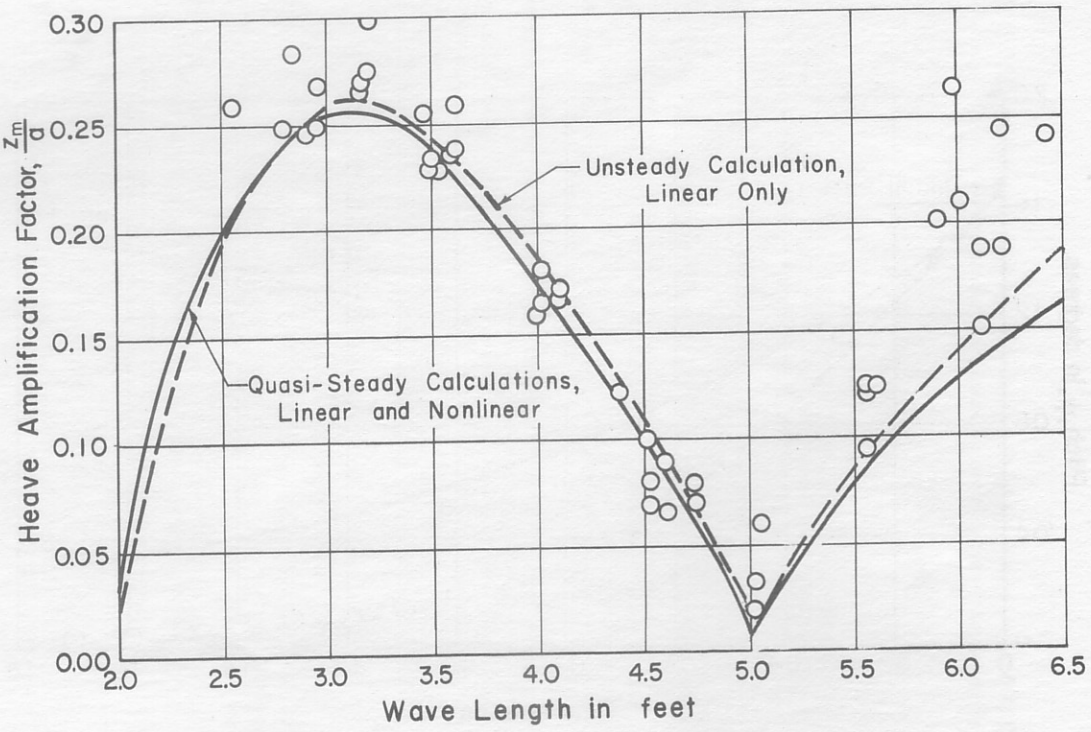

Fig. 6 - Head-Seas Heave Amplification Factor, V = 5 fps

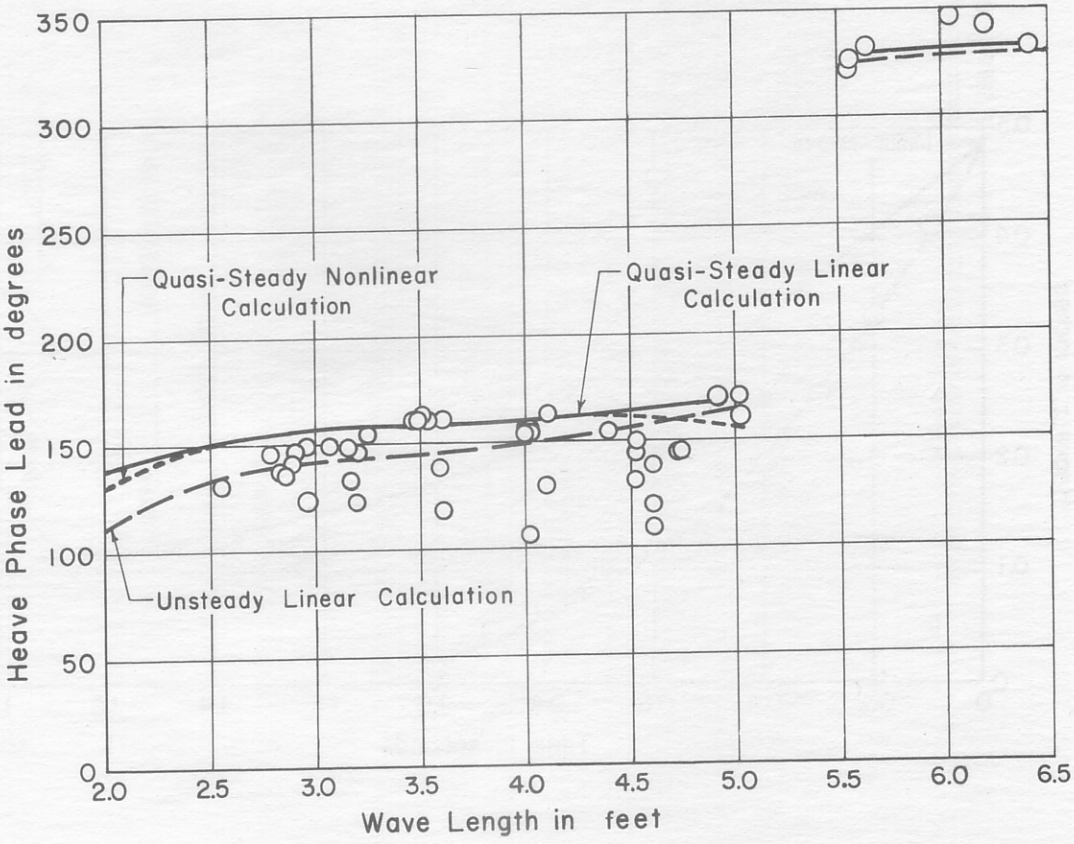

Fig. 7 - Head-Seas Heave Phase Lead, V = 5 fps

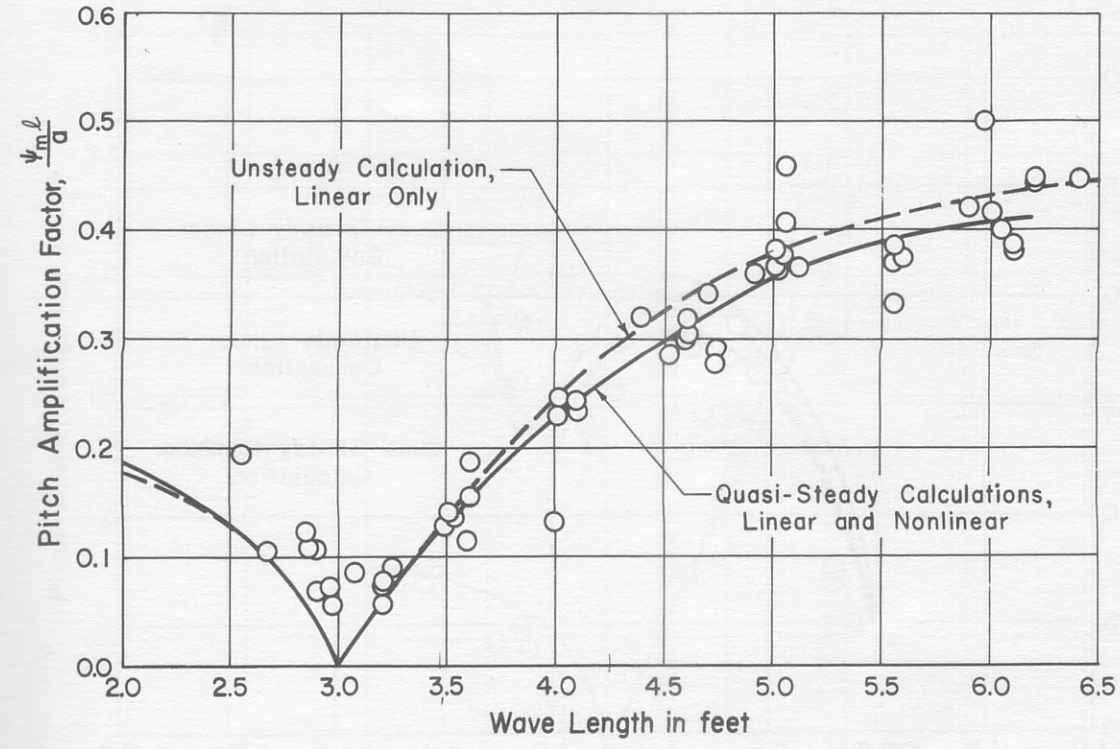

Fig. 8 - Head-Seas Pitch Amplification Factor, V = 5 fps

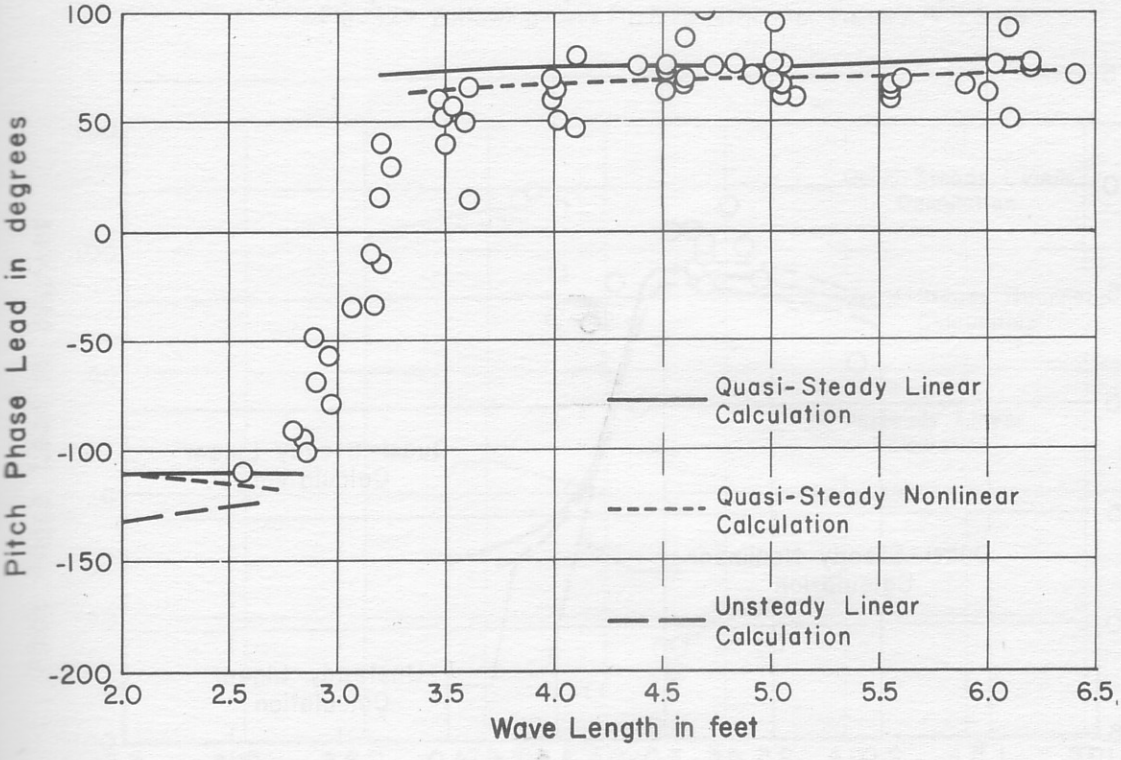

Fig. 9 - Head-Seas Pitch Phase Lead, V = 5 fps

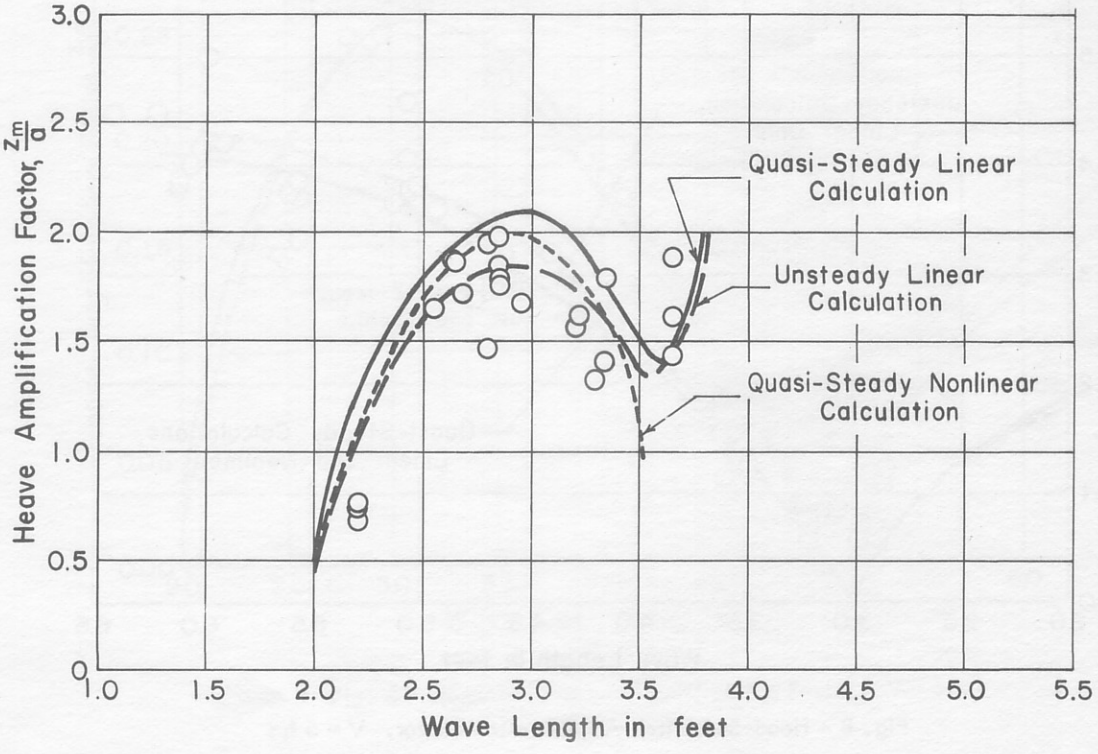

Fig. 10 - Following-Seas Heave Amplification Factor, V = 5 fps

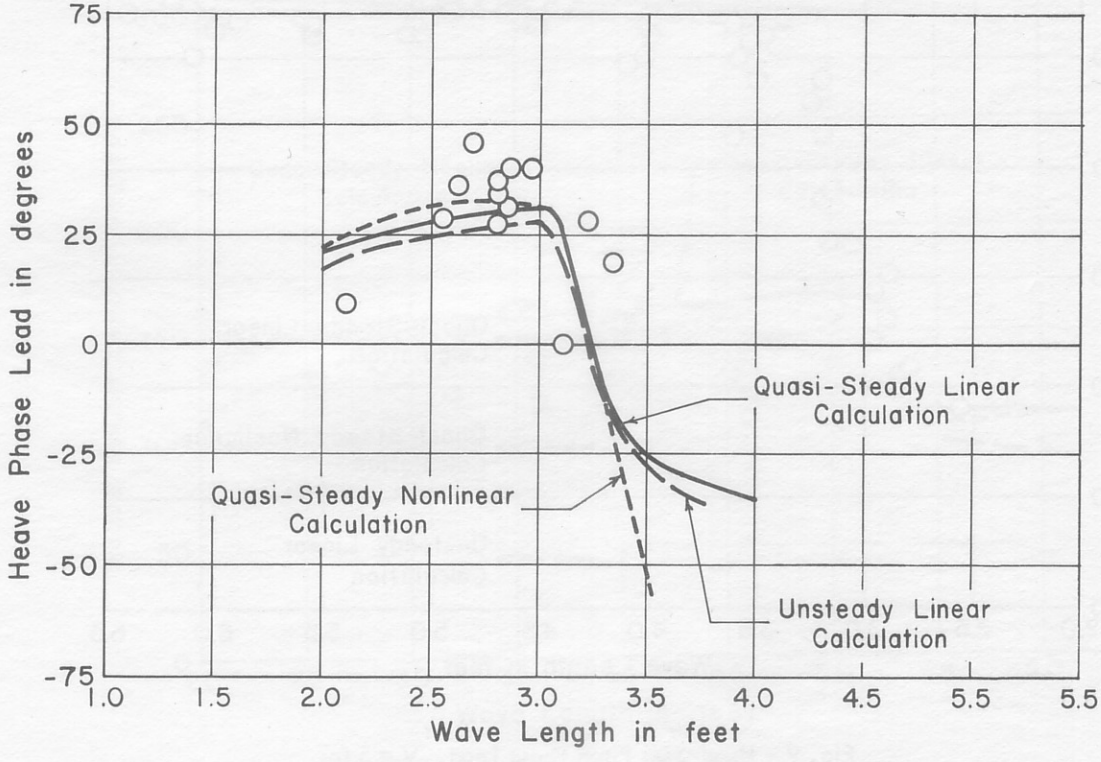

Fig. 11 - Following-Seas Heave Phase Lead, V = 5 fps

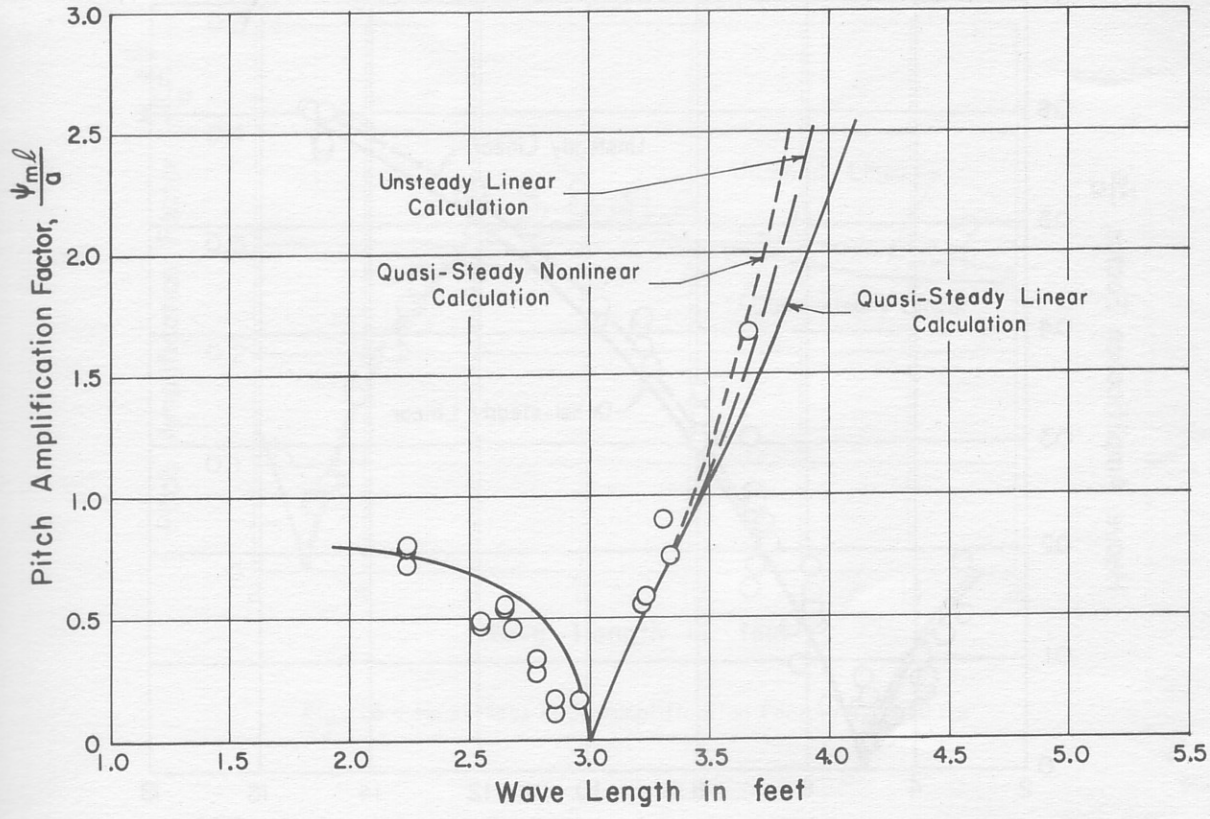

Fig. 12 - Following-Seas Pitch Amplification Factor, V = 5 fps

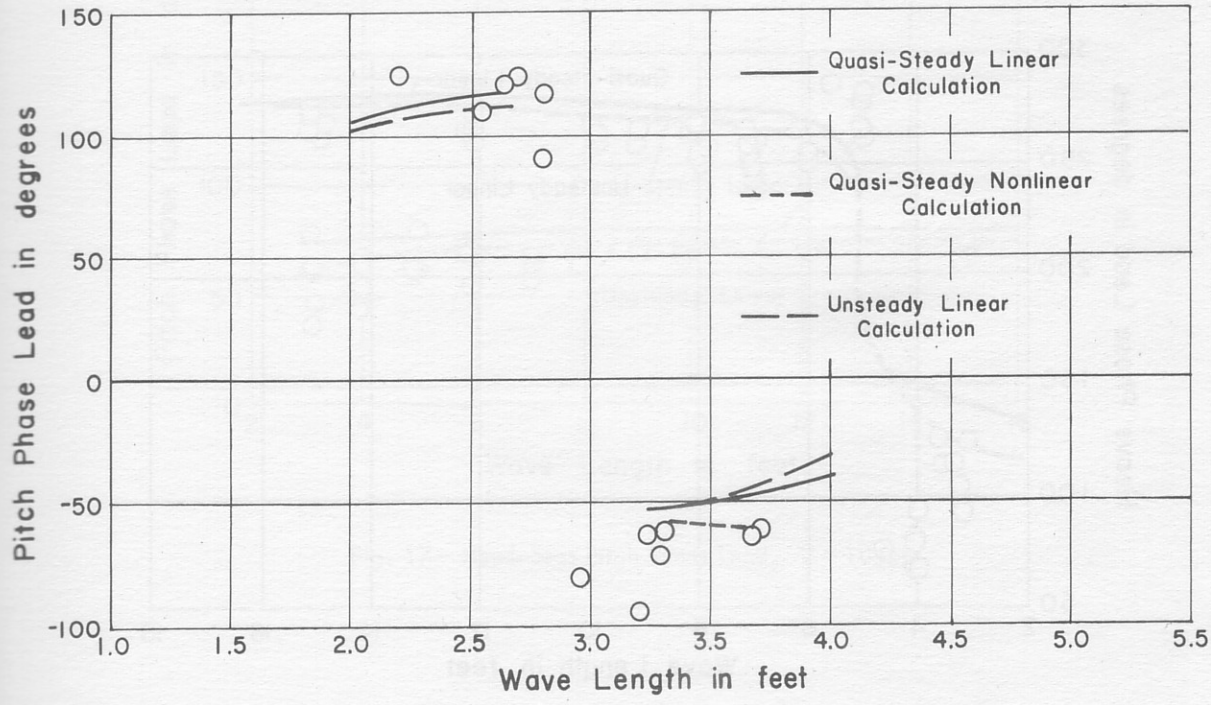

Fig. 13 - Following-Seas Pitch Phase Lead, V = 5 fps

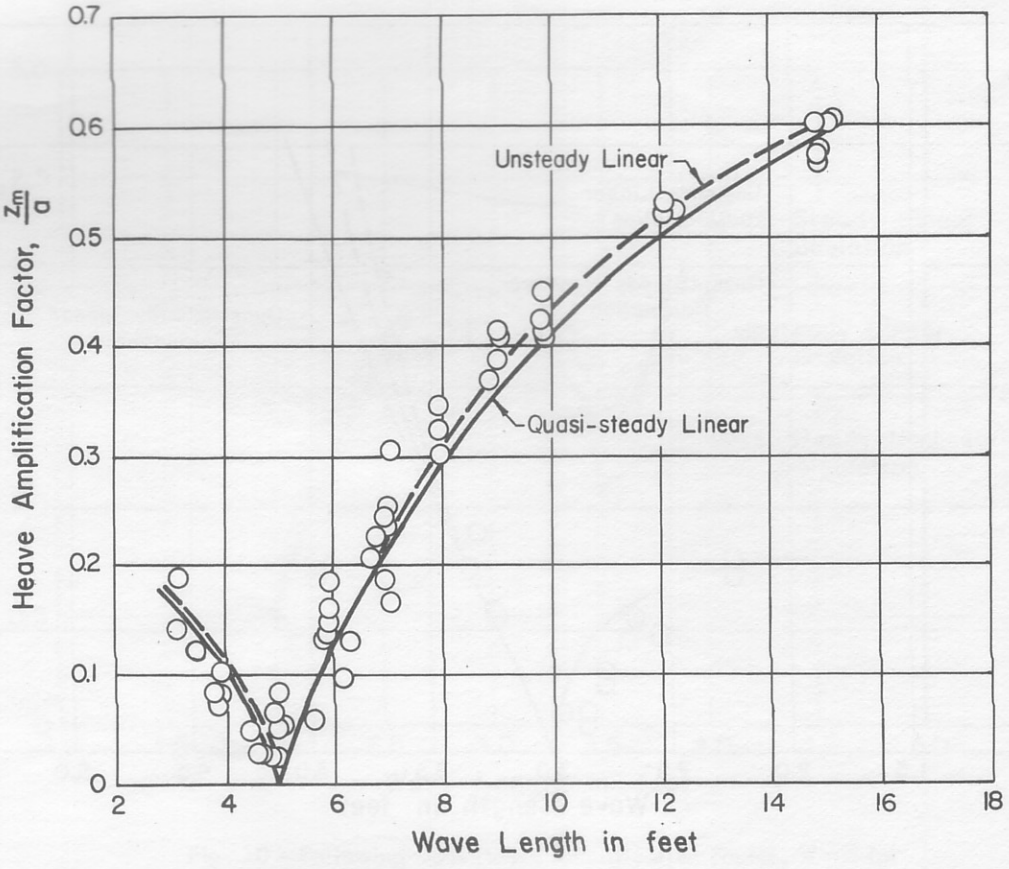

Fig. 14 - Head-Seas Heave Amplification Factor, V = 10 fps

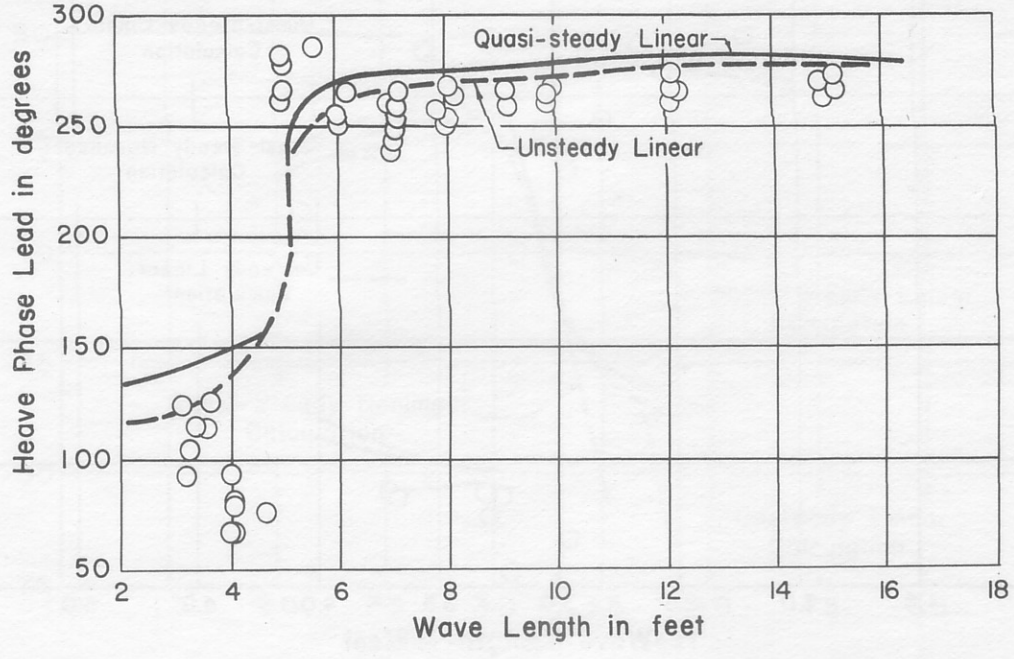

Fig. 15 - Head-Seas Heave Phase Lead, V = 10 fps

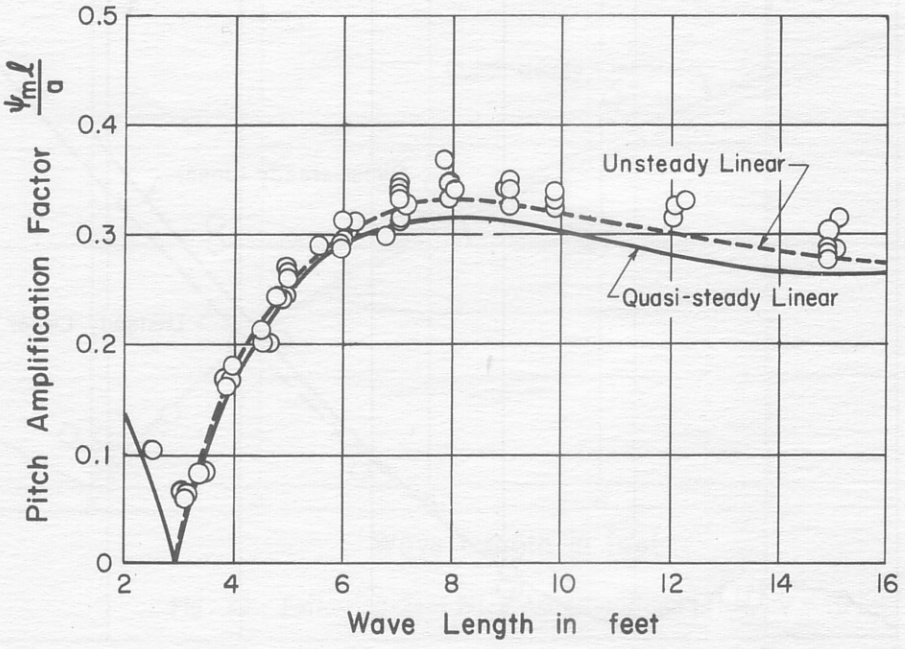

Fig. 16 - Head-Seas Pitch Amplification Factor, V = 10 fps

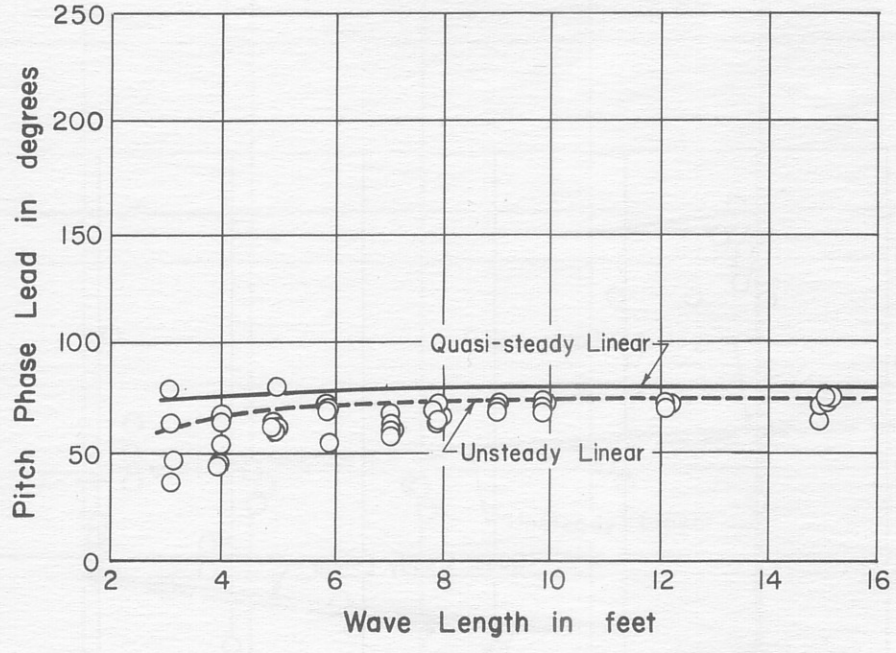

Fig. 17 - Head-Seas Pitch Phase Lead, V = 10 fps

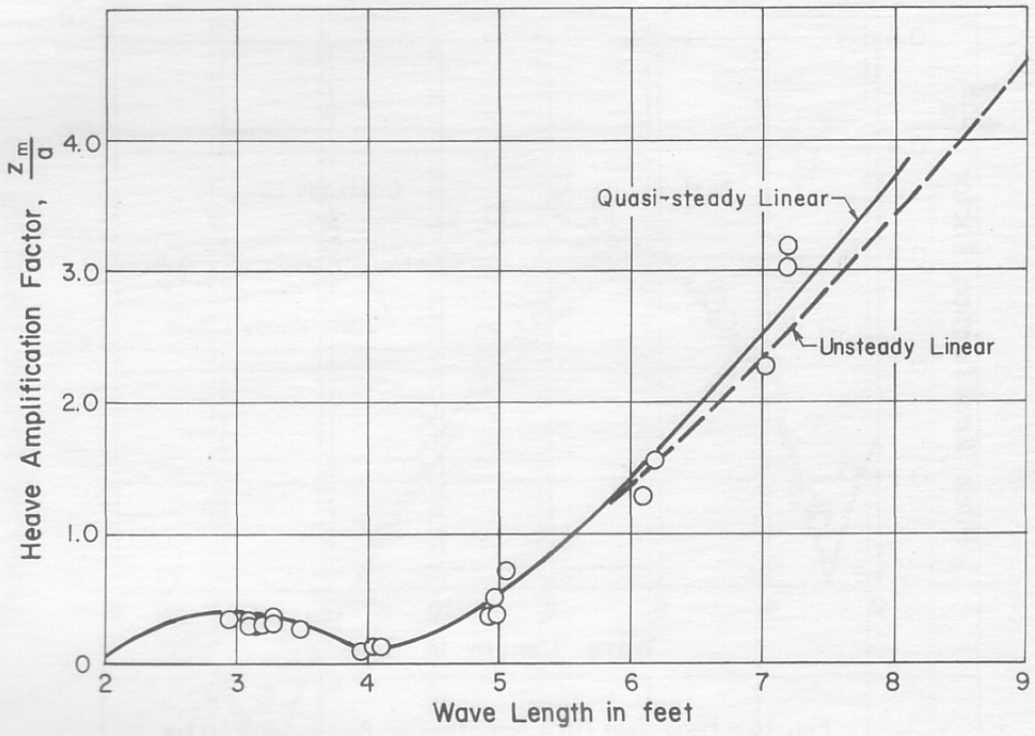

Fig. 18 - Following-Seas Heave Amplification Factor, V = 10 fps

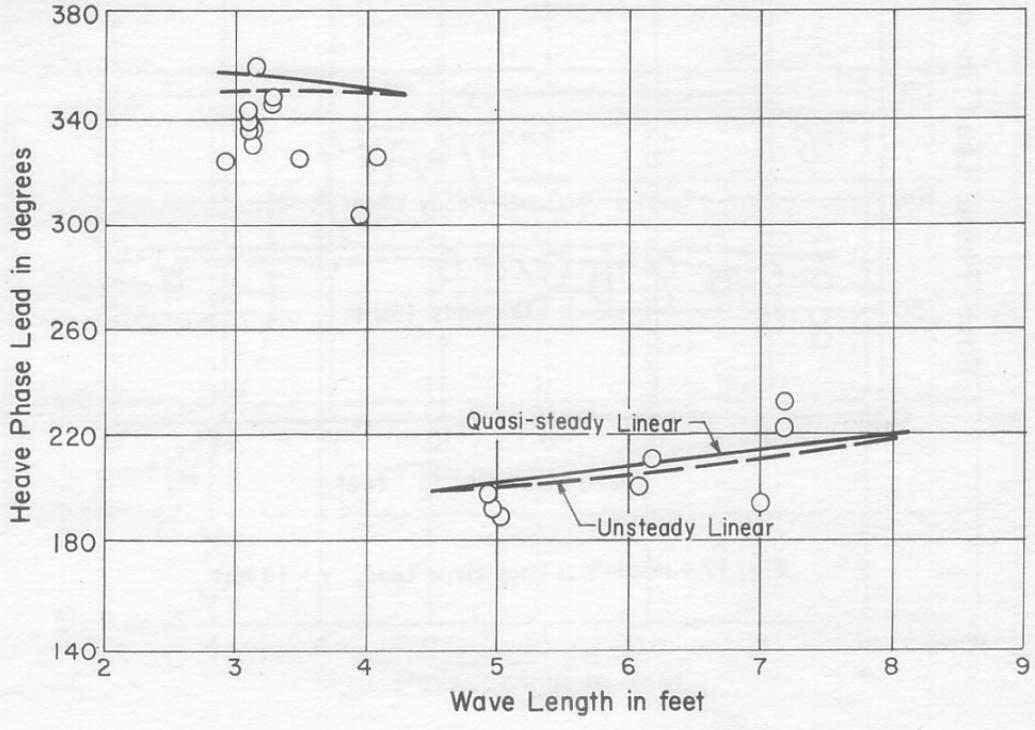

Fig. 19 - Following-Seas Heave Phase Lead, V = 10 fps

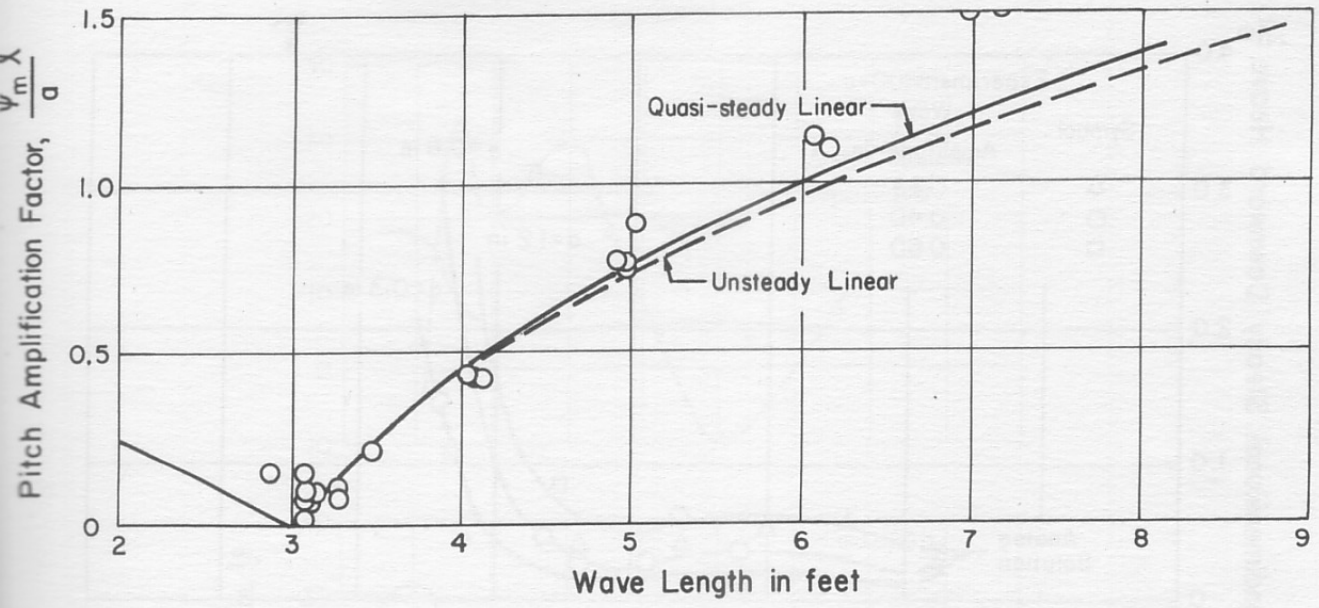

Fig. 20 - Following-Seas Pitch Amplification Factor, V = 10 fps

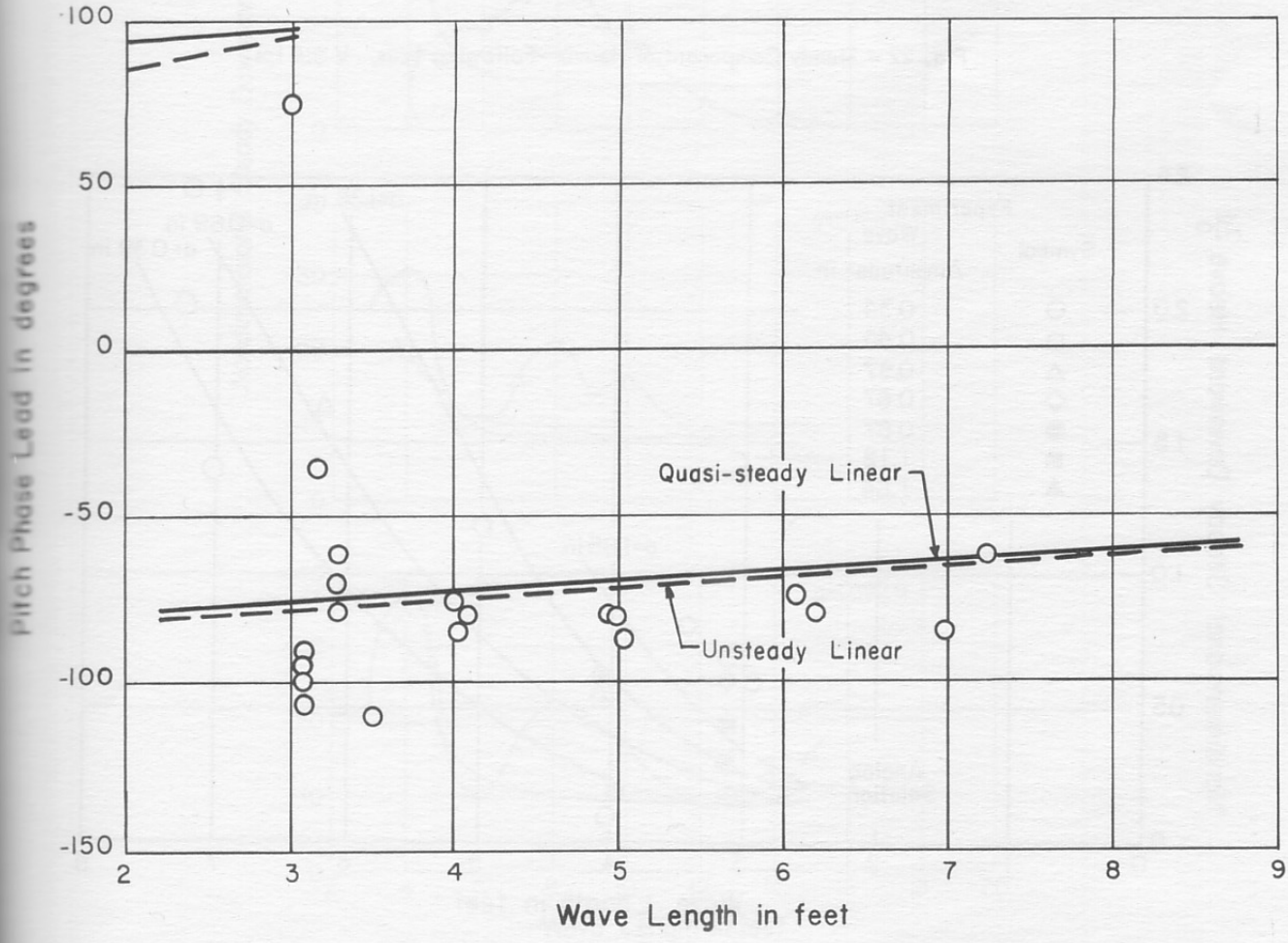

Fig. 21 - Following-Seas Pitch Phase Lead, V = 10 fps

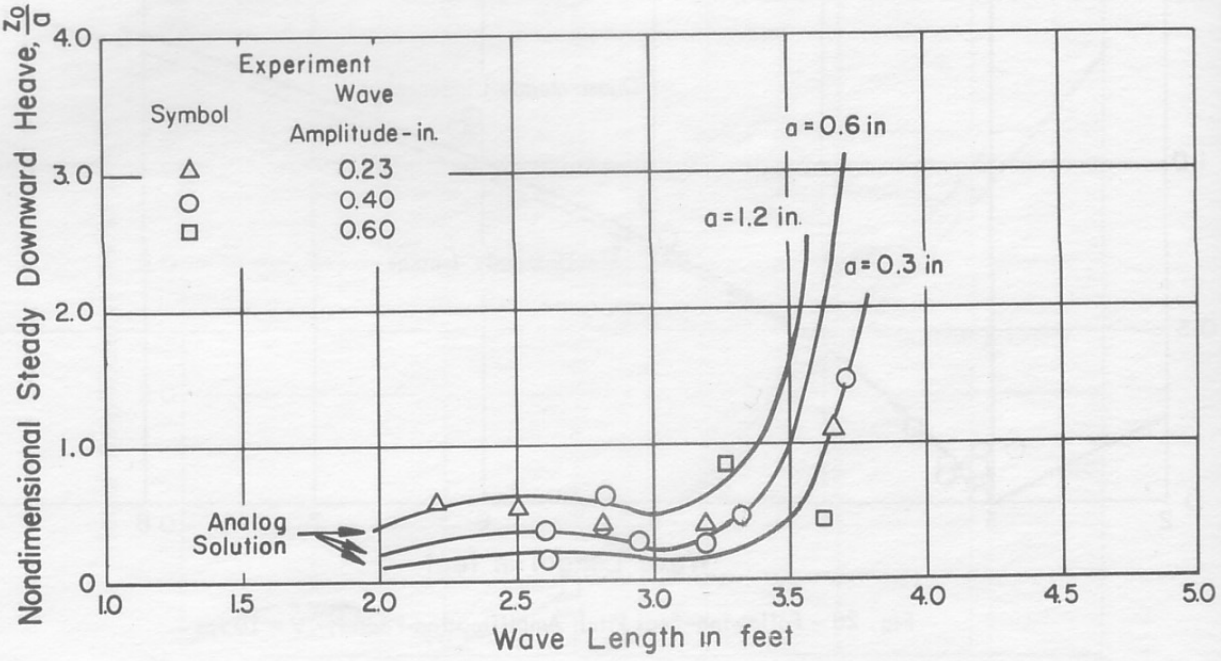

Fig. 22 - Steady Component of Heave--Following Seas, V = 5 fps

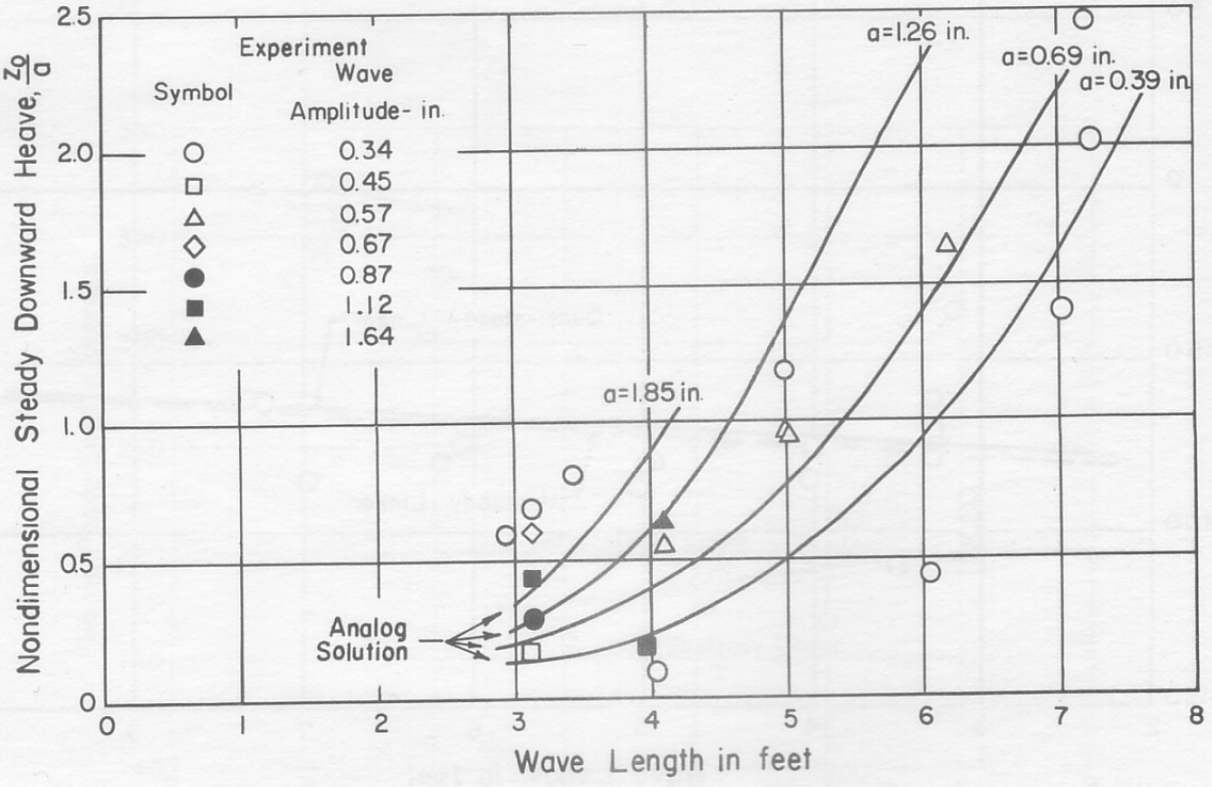

Fig. 23 - Steady Component of Heave--Following Seas, V = 10 fps

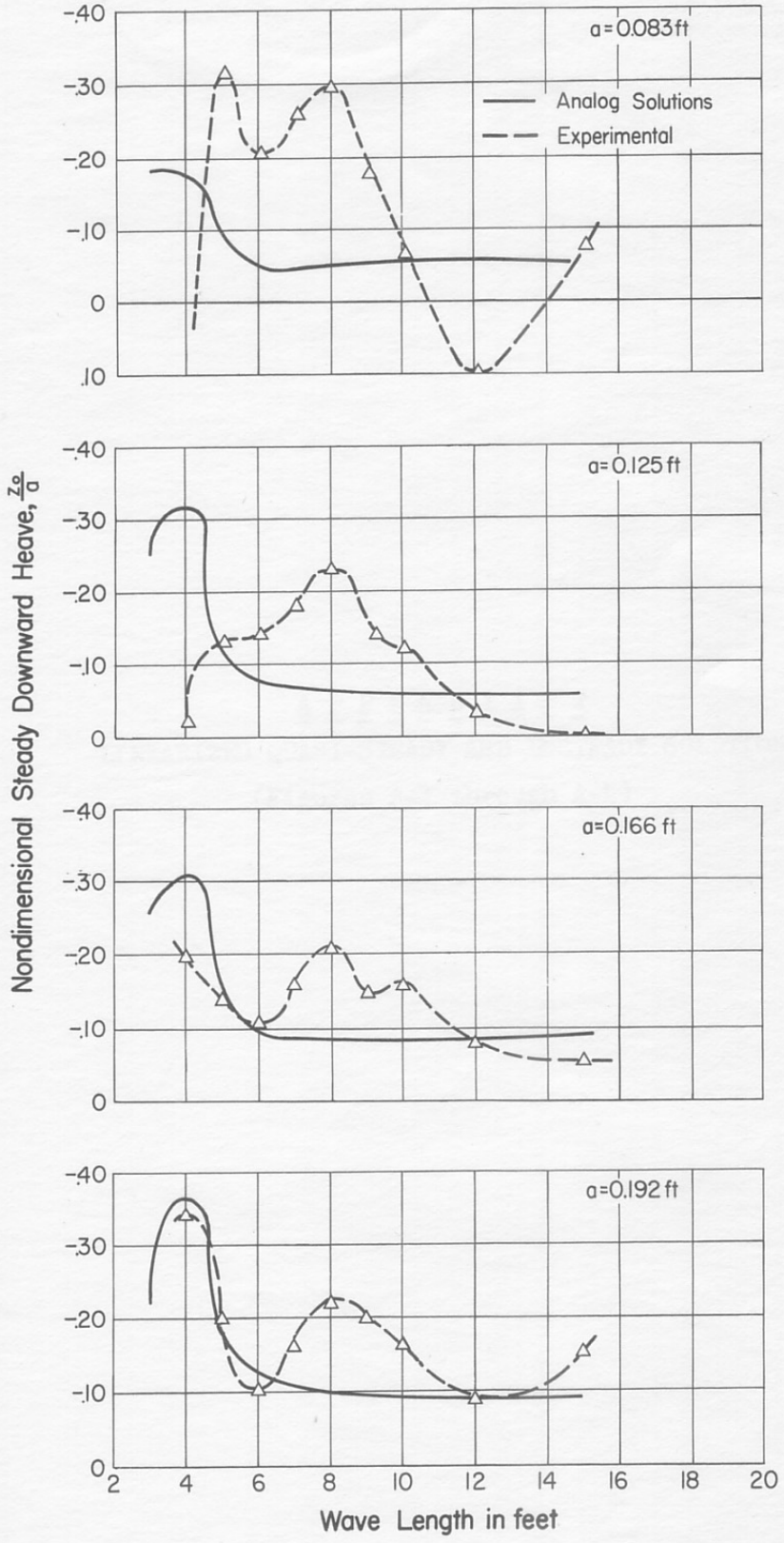

Fig. 24 - Steady Component of Heave--Head Seas, V = 10 fps

A P P E N D I X A

LINEARIZED QUASI-STEADY AND UNSTEADY SOLUTIONS

(Figures A-1 through A-4)

APPENDIX A

LINEARIZED QUASI-STEADY AND UNSTEADY SOLUTIONS

A. Quasi-Steady Equations and Solutions

The linearized equations and solutions are presented here for reference purposes. The linearized equations were obtained by expanding Eqs. (3) and (4), and then omitting all squared terms and cross products of the variables Z, ψ, and a. The results of this simplification are

$$\ddot{Z} + A'\dot{Z} + BZ + C_o\dot{\psi} + C\psi = D\cos \nu t + E \sin \nu t \qquad \text{(A-1)}$$

$$\ddot{\psi} + F\dot{\psi} + G\psi + G_o\dot{Z} + G_1 Z = H\cos \nu t + J \sin \nu t \qquad \text{(A-2)}$$

where $A' = \sum_{f,a} dB'/mV$

$$B = \sum_{f,a} B_o/m$$

$$C_o = 1/mV\,[\ell_f B'_f d_f - \ell_a B'_a d_a]$$

$$C = 1/m\left\{-\sum_{f,a} dB' - \ell_a B_{o_a} + \ell_f B_{o_f}\right\}$$

$$D = 1/m\left\{\sum_{f,a} a B_o \cos k\ell \mp \frac{d_f B'_f a\omega A_f \sin k\ell_f}{V} \mp \frac{d_a B'_a a\omega A_a \sin k\ell_a}{V}\right\}$$

$$E = 1/m\left\{\sum_{f,a} \mp \frac{d B' a \omega A}{V} \cos k\ell + a B_{o_a} \sin k\ell_a - aB_{o_f} \sin k\ell_f\right\}$$

$$F = \sum_{f,a} \frac{d\ell^2 B'}{IV}$$

$$G = \sum_{f,a} \frac{\ell^2 B_o}{I} + 1/I\,[d_a \ell_a B'_a - d_f \ell_f B'_f]$$

$$G_o = 1/IV \left\{ d_f \ell_f B'_f - d_a \ell_a B'_a \right\}$$

$$G_1 = 1/I \left[\ell_f B_{o_f} - \ell_a B_{o_a} \right]$$

$$H = 1/I \left[\mp \sum_{f,a} \frac{d\ell \, B' \, a\omega A}{V} \sin k\ell + a \ell_f B_{o_f} \cos k\ell_f \right.$$

$$\left. - a B_{o_a} \ell_a \cos k\ell_a \right]$$

$$J = 1/I \left[\mp \frac{d_f \ell_f B'_f \, a\omega A_f \cos k\ell_f}{V} \pm \frac{d_a \ell_a B'_a \, a\omega A_a \cos k\ell_a}{V} \right.$$

$$\left. - \sum_{f,a} a \ell B_o \sin k\ell \right]$$

For the configuration in this report with two identical hydrofoils spaced at equal distances from the center of gravity flying with zero trim, one can let

$$\ell_f = \ell_a \qquad A_f = A_a$$

$$d_f = d_a$$

It is then seen that

$$C_o = G_o = G_1 = 0$$

The solutions of the linearized equations can be divided into two parts: the steady-state solution created by the periodic forcing function and the damped transient solution depending on the initial conditions. The first will be considered at this time. The steady-state solutions are

$$\psi = A_1 \cos (\nu t - \phi_\psi) \tag{A-3}$$

$$Z = A_2 \cos (\nu t - \phi_Z) \tag{A-4}$$

where

$$A_1 = \left[\frac{H^2 + J^2}{(G - \nu^2)^2 + F^2\nu^2} \right]^{1/2}$$

$$\phi_\psi = \tan^{-1}\left[\frac{HF\nu - J(G - \nu^2)}{JF\nu + H(G - \nu^2)} \right]$$

$$A_2 = \left[\frac{\gamma^2 + \delta^2}{A^2\nu^2 + (B - \nu^2)^2} \right]^{1/2}$$

$$\phi_Z = \tan^{-1}\left[\frac{\gamma A'\nu + \delta(B - \nu^2)}{\gamma(B - \nu^2) - A'\nu\delta} \right]$$

$$\gamma = CM + D$$

$$\delta = CN + E$$

$$M = \frac{JF\nu + H(G - \nu^2)}{F^2\nu^2 + (G - \nu^2)^2}$$

$$N = \frac{HF\nu - J(G - \nu^2)}{F^2\nu^2 + (G - \nu^2)^2}$$

Coefficients A' through J have been previously defined. The wave amplitude, a, may be factored from the right side of the equations, indicating that the amplification factors are independent of the wave amplitude. Numerical values of the coefficients for tandem "V" foil configuration are given in Tables A-I and A-II for the two towing velocities. Coefficients D, E, H, and J depend on the wave characteristics, and E and H are different for head and following seas. The values in Table A-II are for following seas. Head seas will require a change in sign. For these computations, only the first term was retained in the series expansion for the exponential decay factor, A.

TABLE A-I

Coefficient	Velocity, fps 5	10
A'	62.5	88
B	58.5	77.3
C	312	880
F	117	168.5
G	109.9	148

TABLE A-II

Forcing Function Coefficients

	Velocity = 5 fps				Velocity = 10 fps			
λ	D	E	H	J	D	E	H	J
2	0	0	-391	+73.20	0	0	-635	+99
3	-58.5	-303.5	0	0	-77.4	-483	0	0
4	-41.5	-104.5	132	-51.75	-54.7	-325	412	-69.7
5	-18.05	-88.5	339.5	-69.6	-23.9	-134	522	-94.0
6	0	0	342.0	-73.25	0	0	530	-98.7
7	13.6	30.8	161.2	-71.3	17.2	88	489	-96.1
8	24.3	52.8	147.0	-67.6	29.8	145	443	-91.0
9	29.2	61.5	133.9	-63.5	38.9	183	400	-85.5
10					45.5	203	356	-80.0
11					50.6	220	326	-74.6
12					54.7	231	294	-69.7
13					58.0	233	264	-65.4
14					60.6	242	246	-61.5
15					62.5	241	222	-58.0

B. Transient Solutions and Stability

It was of interest to determine the stability of the configuration for the higher towing velocity. For this purpose, the homogeneous quasi-steady linearized equations were used (Eqs. (A-1) and (A-2) with forcing functions equal to zero). If solutions of the form $Z = \bar{Z} e^{\sigma t}$, $\psi = \bar{\psi} e^{\sigma t}$ are

assumed to exist, then for the existence of nontrivial solutions it is necessary that the characteristic equation

$$\sigma^4 + a_1\sigma^3 + a_2\sigma^2 + a_3\sigma + a_4 = 0 \qquad \text{(A-5)}$$

where $a_1 = A' + F$

$a_2 = A'F + B + G$

$a_3 = A'G + BF$

$a_4 = BG$

The stability is guaranteed when the roots of the quartic (A-5) are negative or at most complex with negative real parts. This will be true if all the coefficients are greater than zero, and if Routh's discriminant

$$a_1 a_2 a_3 - a_3^2 - a_1^2 a_3 a_4 > 0$$

The numerical values of the coefficients and the roots are given in Table A-III.

TABLE A-III

Coefficient or Root	Velocity, fps 5	10
a_1	179	256.5
a_2	7440	15,017
a_3	13,680	26,026
a_4	6430	11,467
σ_1	-0.95	-0.89
σ_2	-0.95	-0.89
σ_3	-61.3	-87.1
σ_4	-115.9	-167.6

It can be seen that the configuration is stable, as the above requirements for stability are satisfied. The roots also give information regarding the transient response of the system. The larger roots indicate extreme damping of any disturbance, and for purposes of calculation these terms were assumed negligible. The calculated transient response based on specified initial conditions has been compared with theory in Section IV.

C. Unsteady Linearized Equations and Solution

Unsteadiness was assumed to affect the lift on the foil through wake vorticity, added mass, and nonuniformity of the orbital motion over the chord. From analogy to the problem of oscillatory air foils in aerodynamics, it is assumed that solutions exist of the form

$$Z = \mathcal{Z}\, e^{i\nu t}$$

$$\psi = \Psi\, e^{i\nu t}$$

where both $\mathcal{Z}$ and Ψ may be complex quantities. The expression for the lift was then written

$$L = \rho V^2 (b \cot \mu) \frac{c'd}{V} D [V\Psi - i\nu\mathcal{Z} - i\nu\, \delta_\ell \Psi]\, e^{i\nu t} \pm \rho V^2 (b \cot \mu)$$

$$\frac{ia\omega A\, c'd}{V} E\, e^{i(k\delta_\ell + \nu t)} - \rho V^2 c_o (b \cot \mu)$$

$$[\mathcal{Z} + \delta_\ell \Psi - ae^{ik\delta_\ell}]\, e^{i\nu t} \qquad \text{(A-6)}$$

D and E are unsteady force functions defined by

$$D = [C(\nu b/2V) + i\nu b/4V] = \mathcal{X} e^{i\zeta}$$

$$E = [J_o (kb/2) - iJ_1 (kb/2)]\, C(\nu b/2V) + i(V[1 \pm C/V])\, J_1 (kb/2)] = \mathcal{Y} e^{i\theta}$$

$$C(\nu b/2V) = F(\nu b/2V) + iG(\nu b/2V) \qquad \text{(Theodorsen's function)}$$

J_o and J_1 are the Bessel functions of the first kind of order zero and one respectively. Plots of C, D, and E are shown in Figs. A-1 through A-3 for the range of conditions of interest. The Theodorsen function was plotted from values given in Reference [9]. The functions D and E go to one for the quasi-steady case. The complex function, D, can be divided into two parts: the wake vorticity correction, C, and the added mass correction. Thus the difference between the functions C and D for a particular reduced frequency represents the effect of added mass. The Theodorsen function, C, approaches the value 1/2 for large $\nu b/2V$, whereas D will continue to change, indicating continued added mass effects. For a given foil

and velocity, the wave length will increase with decreasing reduced frequency. Therefore, added mass effects are more predominate for the smaller wave lengths.

The unsteady force function, E, corrects for nonuniformity of the velocity over the chord. As a term with a double sign appears, this function will attain different values for head and following seas. These curves are shown in Fig. A-3 for a towing velocity of 10 fps.

The unsteady linearized solutions require considerably more effort in numerical computation than the quasi-steady solutions. If the expression for the lift in Eq. (A-6) is placed in the equations of motion

$$m\ddot{Z} = \sum_{f,a} L$$

$$I\ddot{\psi} = \sum_{f,a} \delta \ell L$$

the results are

$$\frac{-B'dD}{V}[V\Psi - i\nu Z] \mp \frac{ia\omega AB'dE}{V}\cos k\ell + B_o[Z - a\cos k\ell] = mZ\nu^2/2 \tag{A-7}$$

$$\frac{B'dD}{V} i\nu\ell\Psi \pm \frac{a\omega AB'dE}{V}\sin k\ell + B_o[\ell\Psi - ai\sin k\ell] = \frac{I\Psi\nu^2}{2\ell} \tag{A-8}$$

It is now necessary to solve Eqs. (A-7) and (A-8) for Z and Ψ, recognizing that the unsteady force functions D and E are complex quantities. As the pitch Eq. (A-8) does not contain the heave, Z, it can easily be solved for Ψ. The heave equation is then solved in terms of Ψ. It is thus assumed that numerical values of the pitch for a particular set of conditions will be available for the heave computation. The solutions are then given by

$$\psi = \Psi e^{i\nu t} = T_1 e^{i(\nu t + \sigma)} \tag{A-9}$$

where $T_1 = \frac{|\sin k\ell|}{C}[C_1^2 + C_2^2]^{1/2}$

$\sigma = \tan^{-1} C_2/C_1$

$$\beta = aB_o$$

$$\gamma = I\nu^2/2\ell - B_o\ell$$

$$\epsilon = B'd\nu\ell/V$$

$$\eta = \pm \frac{a\omega A_o B'd}{V}$$

$$D = Xe^{i\zeta}$$

$$E = Ye^{i\theta}$$

$$A_1 = \gamma^2 + (\epsilon X^2) \cos 2$$

$$A_2 = (\epsilon X)^2 \sin 2$$

$$C = \left\{ A_1^{\,2} + A_2^{\,2} \right\} 1/2$$

$$A_3 = \eta Y \gamma \cos\theta + \beta\epsilon X \cos\zeta - \eta\epsilon XY \sin(\theta + \zeta)$$

$$A_4 = \eta Y \gamma \sin\theta + \beta\epsilon X \sin\zeta + \eta\epsilon XY \cos(\theta + \zeta) - \beta\gamma$$

$$C_1 = A_3 \cos\xi + A_4 \sin\xi$$

$$C_2 = A_4 \cos\xi - A_3 \sin\xi$$

$$\xi = \tan^{-1} A_2/A_1$$

Equation (A-7) is solved in terms of T_1 and σ.

$$Z = \sum e^{i\nu t} = U/W\, e^{i(\nu t + \tau)} \qquad \text{(A-10)}$$

where $U = \sqrt{C_3^{\,2} + C_4^{\,2}}$

$$W = \sqrt{C_5^{\,2} + C_6^{\,2}}$$

$$\tau = \tan^{-1} \frac{C_4 C_5 - C_3 C_6}{C_3 C_5 + C_4 C_6}$$

$$C_3 = -\beta \cos k\ell + \eta Y \cos k\ell \sin\theta - B'd\, XT_1 \cos(\sigma + \zeta)$$

$$C_4 = -\eta Y \cos k\ell \cos\theta - B'd\, XT_1 \sin(\sigma + \zeta)$$

$$C_5 = m\nu^2/2 - B_o + \epsilon X/\ell \sin\zeta$$

$$C_6 = - \epsilon X/\ell \cos\zeta$$

Note that both σ and τ are phase leads. It is assumed in all cases that the real parts of the solutions will be retained.

D. Analog Computer Solutions

Analog computer solutions of the nonlinear equations were necessary to determine the theoretical steady heave component for a towing velocity of 10 fps. A Reeve's Electronic Analog Computer (REAC) was available for these solutions during the latter part of the program. As the linear solutions were previously obtained by hand computation, they were used as a check on the analog linear solutions. The computer consisted of forty operational amplifiers and four independent servo multipliers each with three multiplying potentiometers. Some difficulty was experienced with the block diagram as used by Ogilvie on this particular computer. For this reason, the physical equations were arranged in a slightly different manner.

The quasi-steady nonlinear Eqs. (3) and (4) can be written as

$$\ddot{Z} = C\overline{W} + B\overline{X} + C/d\,[\overline{WX} + \overline{YI}] \qquad \text{(A-11)}$$

$$-\ddot{\psi} = VF\overline{Y}/\ell + G/\ell\,\overline{I} + VF/\ell d\,[\overline{WI} + \overline{YX}] \qquad \text{(A-12)}$$

where $\overline{W} = \psi - \dot{Z}/V + U \sin \nu t$

$\overline{X} = - Z + W \cos \nu t$

$\overline{Y} = \ell/V\,\dot{\psi} + T \cos \nu t$

$\overline{I} = \ell\,\psi + X \sin \nu t$

$T = \pm\omega\, A/V \sin k\ell$

$U = \mp\omega\, A/V \cos k\ell$

$W = \cos k\ell$

$X = \sin k\ell$

The above equations were written in terms of previously defined quantities whenever possible. The computer equations for a computer time $r = 10\,t$ are shown on the block diagramin Fig. A-4 for conditions at a towing velocity of 10 fps and head seas. As the motions for following seas were

greater than for head seas, it was necessary to reduce the level of the variables by a factor of 3 on the integrators to prevent overloading. This also required a change in amplifier gains in the summers and a corresponding change with potentiometer settings. If the angle of attack and depth of submergence of each foil are desired, they can be found easily by summing the variables

$$a_f = \overline{W} - \overline{Y} \qquad \beta_f = \overline{X} - \overline{I}$$

$$a_a = \overline{W} + \overline{Y} \qquad \beta_a = \overline{X} + \overline{I}$$

The potentiometer settings for head seas in terms of the coefficients are given in Table A-IV.

TABLE A-IV

Pot.	Setting	Pot.	Setting	Pot.	Setting	Pot.	Setting
1	0.3	6	$3\ell/V$	11	B/300	16	VF/9000 ℓd
2	7.5/V	7	$0.75\lvert T\rvert$	12	C/9000 d	17	VF/9000 ℓd
3	$0.75\lvert U\rvert$	8	$0.75\lvert X\rvert$	13	C/9000 d	18*	ν/100
4	0.75	9	0.3ℓ	14	VF/1200 ℓ	19*	ν/100
5	$0.75\lvert W\rvert$	10	c/1200	15	G/300 ℓ		

*For $\nu > 10$ and integrator gain at 10. For $\nu < 10$ and integrator gain at 1, multiply these values by 10.

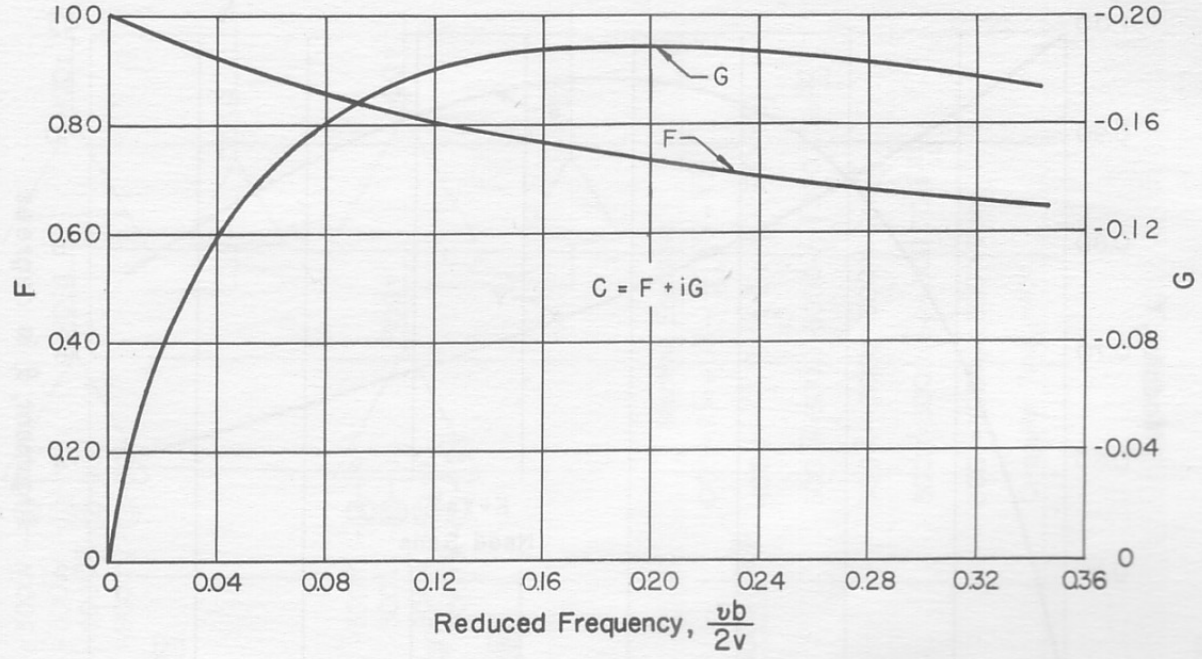

Fig. A-1 – Theodorsen's Function

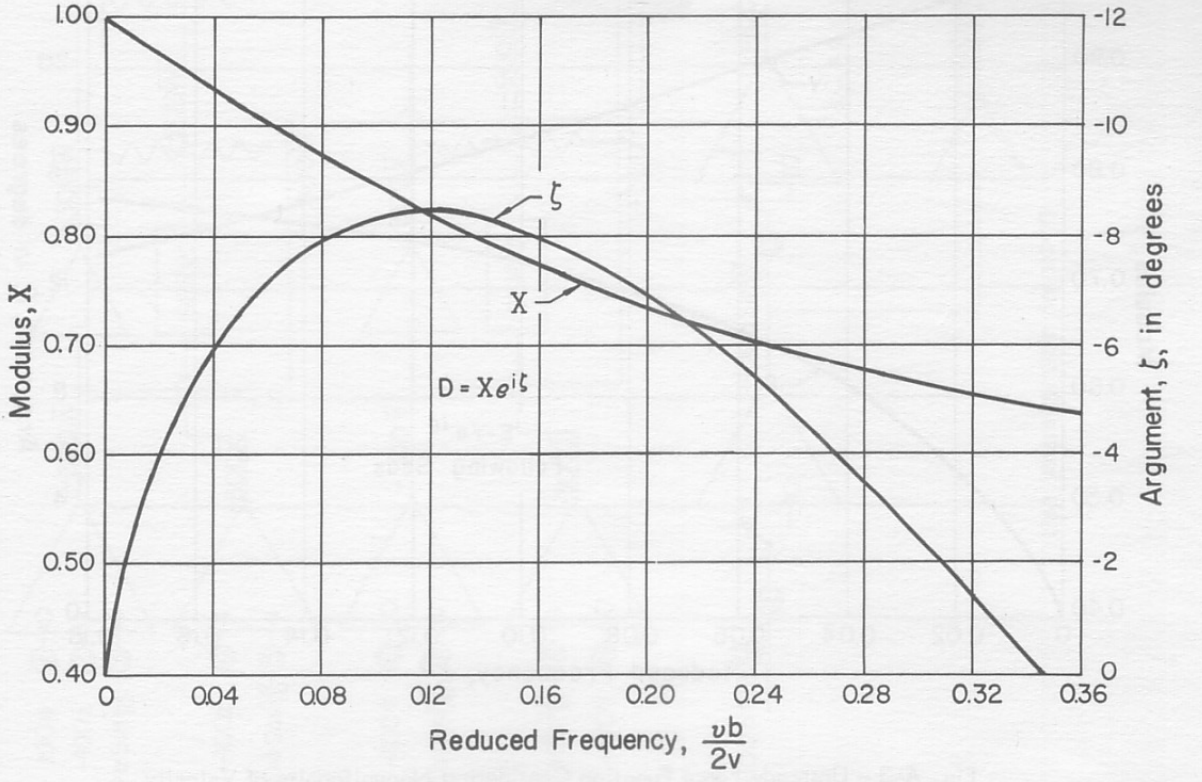

Fig. A-2 – Unsteady Force Function Considering Foil Motions

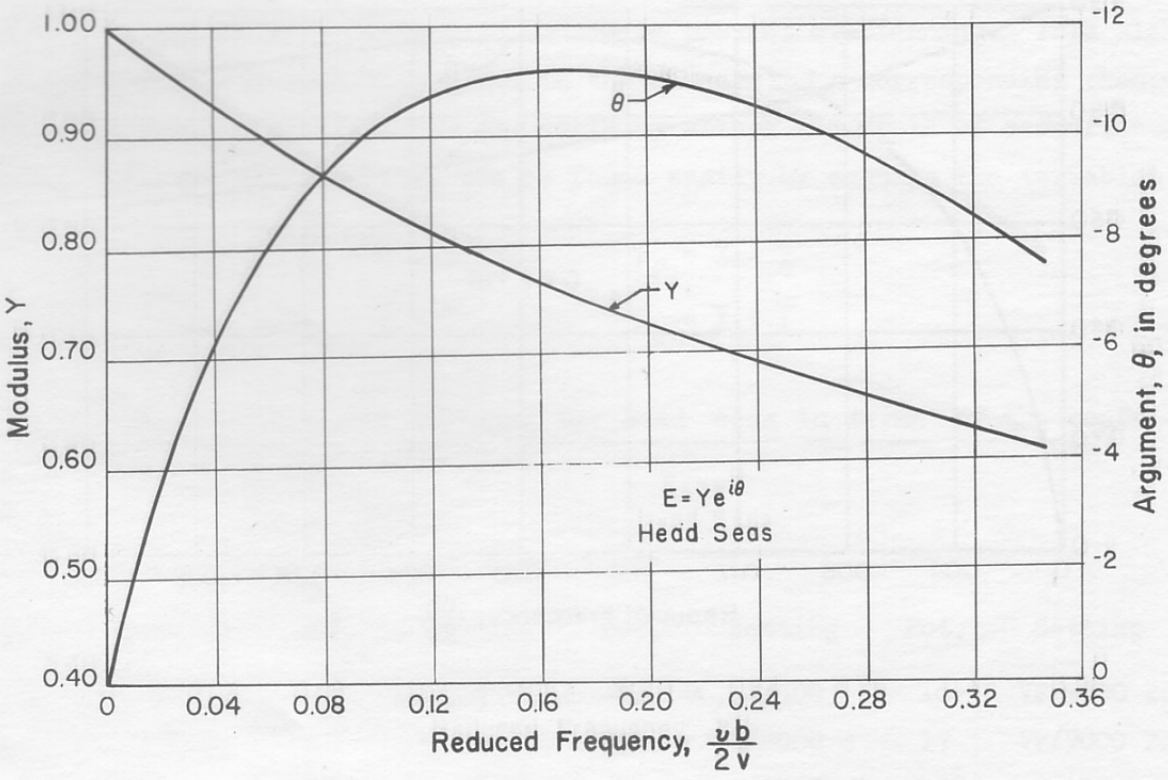

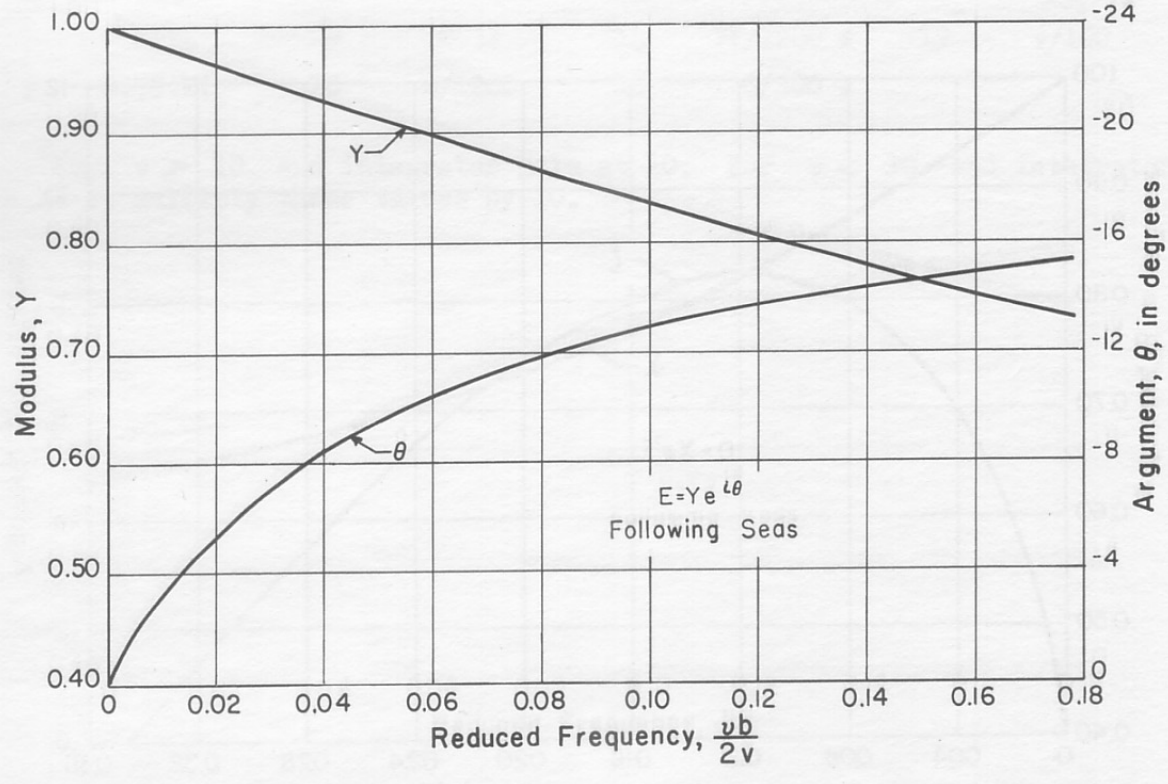

Fig. A-3 – Unsteady Force Function Considering Nonuniformity of Velocity Over Chord

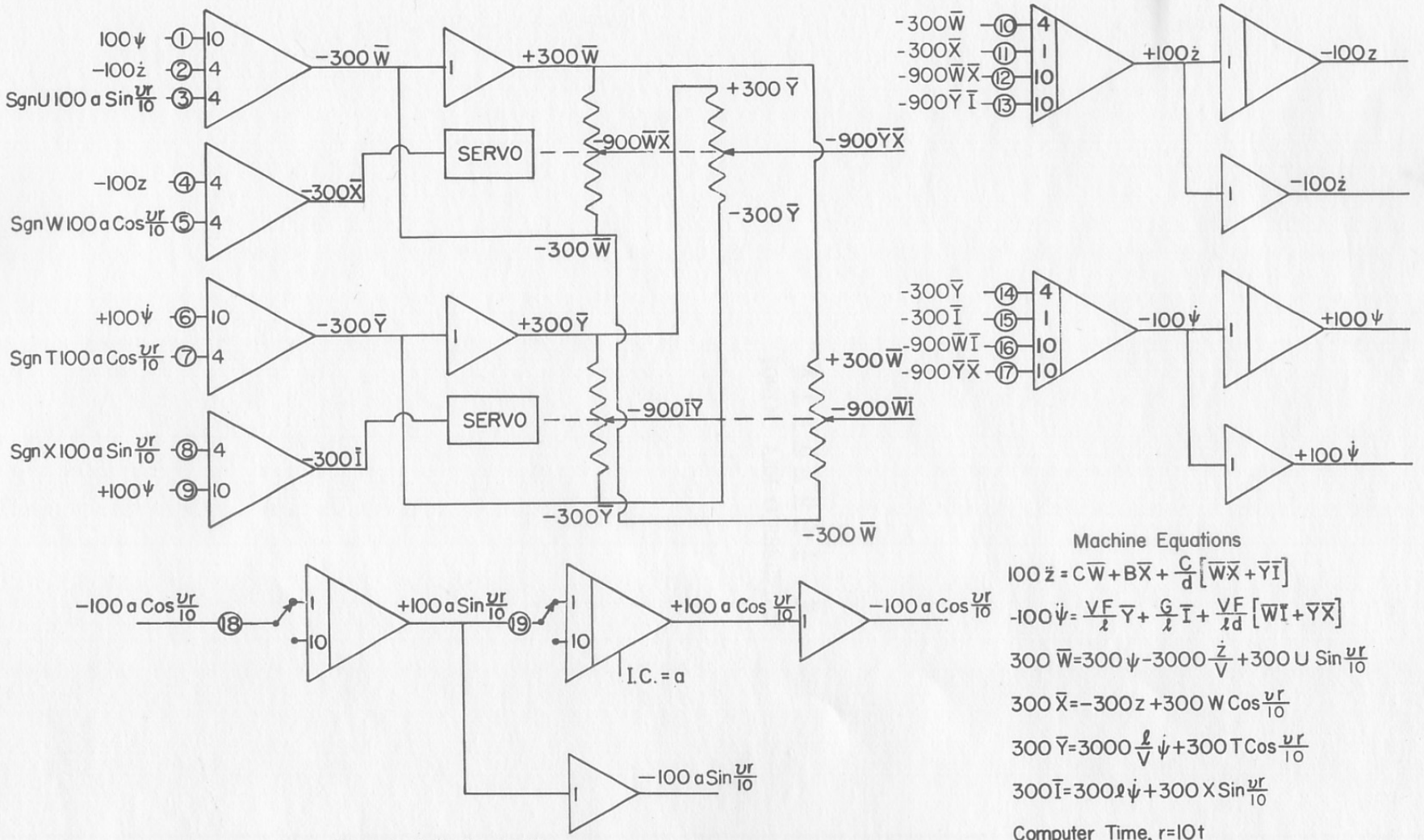

Machine Equations

$$100\ddot{z} = C\bar{W} + B\bar{X} + \frac{C}{d}\left[\bar{W}\bar{X} + \bar{Y}\bar{I}\right]$$

$$-100\ddot{\psi} = \frac{VF}{\ell}\bar{Y} + \frac{G}{\ell}\bar{I} + \frac{VF}{\ell d}\left[\bar{W}\bar{I} + \bar{Y}\bar{X}\right]$$

$$300\,\bar{W} = 300\psi - 3000\frac{\dot{z}}{V} + 300\,U\,\mathrm{Sin}\frac{\upsilon r}{10}$$

$$300\,\bar{X} = -300z + 300\,W\,\mathrm{Cos}\frac{\upsilon r}{10}$$

$$300\,\bar{Y} = 3000\frac{\ell}{V}\dot{\psi} + 300\,T\,\mathrm{Cos}\frac{\upsilon r}{10}$$

$$300\bar{I} = 300\ell\dot{\psi} + 300\,X\,\mathrm{Sin}\frac{\upsilon r}{10}$$

Computer Time, $r = 10t$

Fig. A-4 – Analog Computer Block Diagram

APPENDIX B

TOWING ARM CORRECTION

APPENDIX B

TOWING ARM CORRECTION

As discussed in Section III-C, the weight of the towing arm was carefully balanced with the counter weight so that none of its weight bore on the craft. However, the inertia of the towing arm should be considered. The correction has been calculated by the method discussed by Leehey and Steele, and reference will be made to Fig. 2.

As the craft is moved through a vertical distance Z, the towing arm will rotate about its axle through an angle θ. The equation describing such motion is

$$T = I\ddot{\theta} \tag{B-1}$$

If the length of the towing arm is ℓ_T, the torque, T, causing the rotation is given by

$$T = (L_f + L_a - W)\,\ell_T \tag{B-2}$$

From the geometry, it can be seen that for small rotations

$$\theta \cong Z/\ell_T$$

or

$$\ddot{\theta} \cong \ddot{Z}/\ell_T \tag{B-3}$$

Then, combining Eqs. (B-1), (B-2), and (B-3),

$$Z = \frac{(L_f + L_a - W)\ell_T^{\,2}}{I} \tag{B-4}$$

The moment of inertia, I, consists of the inertia of the towing arm and that due to the mass of the craft. The moment about the pivot point of the towing arm is desired, and can be obtained by the translation theorem. Thus,

$$m\ddot{Z} = \frac{(L_f + L_a - W)\, m\ell_T^{\,2}}{I_T + m\ell_T^{\,2}} = \frac{(L_f + L_a - W)\, m}{m + I_T/\ell_T^{\,2}} \tag{B-5}$$

This equation is the same as Eqs. (1) and (2) from which the other solutions were derived with the exception of the factor

$$\frac{m}{m + I_T/\ell_T^2}$$

Therefore, to include the effect of the towing arm, it is necessary to multiply coefficients A' through F in Table A-I by this factor.

In the case of the unsteady linearized equations, this correction is applied to the forcing function of the heave equation, thus

$$m\ddot{Z} = \sum_{f,a} L \frac{m}{m + I_T/\ell_T^2} = T_2 \sum_{f,a} L$$

If harmonic solutions are again assumed, it will be seen that the resulting equation for Z will be identical to Eq. (A-6) with the exception of the term

$$B_o - m\nu^2/2T_2$$

The addition of the towing arm correction changes the heave computation only through the term C_5. In general, the influence of this correction is observed more significantly in the phase relationship.

SPONSOR'S DISTRIBUTION LIST FOR TECHNICAL PAPER NO. 30-B

of the St. Anthony Falls Hydraulic Laboratory

Copies	Organization
65	Commanding Officer and Director, David Taylor Model Basin, Washington 7, D. C., Attn: Code 513.
5	Chief of Naval Research, Department of the Navy, Washington 25, D. C., Attn: Code 438 and Code 439.
3	Chief of Naval Operations, Department of the Navy, Washington 25, D. C., Attn: 1 - Code OP-31 1 - Code OP-07 1 - Code OP-34
1	Commanding Officer, Office of Naval Research, Branch Office, 346 Broadway, New York 13, New York.
1	Commanding Officer, Office of Naval Research, Branch Office, The John Crerar Library Building, 10th Floor, 86 East Randolph Street, Chicago 1, Illinois.
1	Mr. R. K. Johnston, Miami Shipbuilding Corporation, 615 S. W. Second Avenue, Miami 36, Florida.
1	Director, U. S. Naval Research Laboratory, Washington 25, D. C.
1	Commandant, U. S. Marine Corps, Department of the Navy, Washington 25, D. C., Attn: G-3.
1	Assistant Chief of Transportation for Military Operations, Department of the Army, Washington, D. C.
1	Director, Army Research Office, Department of the Army, Washington 25, D. C.
1	Secretary, Undersea Warfare Committee, National Research Council, 2101 Constitution Avenue, N. W., Washington, D. C.
1	Mr. J. G. Baker, President, Baker Manufacturing Company, Evansville, Wisconsin.
1	Dr. L. G. Straub, Director, St. Anthony Falls Hydraulic Laboratory, University of Minnesota, Minneapolis 14, Minnesota.
10	Chief, Bureau of Ships, Department of the Navy, Washington 25, D. C., Attn: 2 - Technical Information Branch (Code 335) 1 - Research and Development (Code 300) 1 - Noise Reduction Section (Code 345) 1 - Preliminary Design (Code 420)

Copies	Organization
	1 - Hull Design (Code 440) 1 - Scientific and Research (Code 442) 1 - Boats and Small Craft (Code 449) 1 - Mine, Service and Patrol Craft (Code 526) 1 - Landing Ships, Boats and Amphibious Vehicles (Code 529)
1	Chief, Bureau of Weapons, Department of the Navy, Washington 25, D. C., Attn: Code RRSY.
1	Commanding Officer, Office of Naval Research, Branch Office, 495 Summer Street, Boston 10, Massachusetts.
1	Commanding Officer, Office of Naval Research, Branch Office, 1030 East Green Street, Pasadena 1, California.
2	Commanding Officer, Office of Naval Research, Branch Office, Navy 100, F. P. O., New York, New York.
1	Director, National Aeronautics and Space Administration, 1512 H Street, N. W., Washington 25, D. C.
1	Commandant, U. S. Coast Guard, 1300 E Street, N. W., Washington 25, D. C.
1	Commandant, Marine Corps Schools, Quantico, Virginia, Attn: Marine Corps Development Center.
2	Director of Research and Development, Department of the Air Force, Washington 25, D. C.
1	Director, Weapons Systems Evaluation Group, Office of the Secretary of Defense, Washington 25, D. C.
1	Mr. T. M. Buerman, Gibbs and Cox, Incorporated, 21 West Street, New York 6, New York.
1	Commanding Officer, Office of Naval Research, Branch Office, 1000 Geary Street, San Francisco 9, California.
1	Professor H. A. Schade, Director, Institute of Engineering Research, Department of Engineering, University of California, Berkeley, California.
1	Dr. A. G. Strandhagen, Head, Department of Engineering Mechanics, University of Notre Dame, Notre Dame, Indiana.
1	Mr. W. R. Ryan, Edo Corporation, College Point 56, Long Island, New York.
1	Commander, Air Research and Development Command, P. O. Box 1395, Baltimore 3, Maryland, Attn: Rdtded.

Copies	Organization
10	Commander, Armed Services Technical Information Agency, Arlington Hall Station, Arlington 12, Virginia.
1	Mr. Phillip Eisenberg, President, Hydronautics, Incorporated, 200 Monroe Street, Rockville, Maryland.
1	Officer in Charge, MWDP Contract Supervisory Staff, SACLANT ASW Research Center, APO 19, New York, New York.
1	Dr. R. C. Seamans, Radio Corporation of America, Waltham, Massachusetts.
1	Hydrodynamics Research Laboratory, Consolidated-Vultee Aircraft Corporation, San Diego 12, California.
1	Mr. J. D. Pierson, The Martin Company, Baltimore 3, Maryland.
1	Dynamic Developments, Incorporated, Seaplane Hangar, Midway Avenue, Babylon, Long Island, New York.
1	Dr. M. S. Plessett, Hydrodynamics Laboratory, California Institute of Technology, Pasadena, California.
1	Commanding Officer and Director, U. S. Naval Civil Engineering Laboratory, Port Hueneme, California, Attn: Code L54.
2	Dr. F. H. Todd, Director, National Physical Laboratory, Teddington, Middlesex, England (1 copy for Mr. A. Silverleaf).
1	Davidson Laboratory, Stevens Institute of Technology, Hoboken, New Jersey.
1	Technical Research Group, 2 Aerial Way, Syosset, L. I., New York, N. Y., Attn: Dr. Paul Kaplan.
1	Editor, Engineering Index, Inc., 29 West 39th Street, New York, N. Y.
1	Editor, Applied Mechanics Reviews, Southwest Research Institute, 8500 Culebra Road, San Antonio 6, Texas.
1	Librarian, Institute of Aeronautical Sciences, 2 East 64th Street, New York 21, N. Y.
1	Librarian, Society of Naval Architects and Marine Engineers, 74 Trinity Place, New York 6, N. Y.